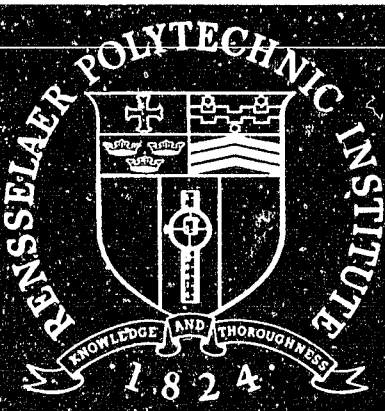

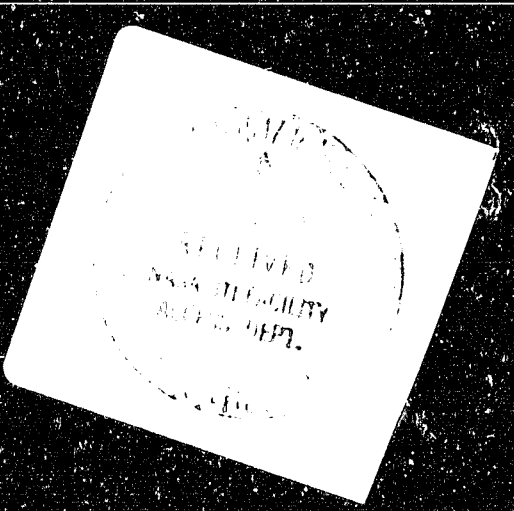

Rensselaer Polytechnic Institute

Troy, New York 12181

RPI TECHNICAL REPORT MP-68

LASER OPTICAL APPRAISAL AND DESIGN OF A PRIME/ROVER INTERFACE

by

James A. Donaldson

A Study Supported by the

NATIONAL AERONAUTICS AND SPACE ADMINISTRATION

under

Grant NSG-7369

and by the

JET PROPULSION LABORATORY

under

Contract 954880

School of Engineering
Rensselaer Polytechnic Institute
Troy, New York

July 1980

CONTENTS

LIST OF TABLES

LIST OF FIGURES

ACKNOWLEDGEMENT

I would like to express my gratitude to: Dr. Stephen Yerazunis whose enthusiasm was contagious; Dr. David Gisser whose encouragement kept me going when completing this project looked impossible; Dr. D. Frederick who provided leadership at a difficult time; Paul Dunn, Gary Coles and Andy Segal whose presence made weeks of fruitless labor bearable; Carl Simchick for help with computer simulation, and Michael Potmesil whose suggestions inspired me to be more thorough.

ABSTRACT

An appraisal of whether to improve the existing multi-laser/multi-detector system was undertaken. This involved studying two features of the elevation scanning mast which prevent the system from meeting desired specifications. These features are: first, the elevation scanning mast has 20 detectors, as opposed to the desired 40. This influences the system's overall resolution. Second, the mirror shaft encoder's finite resolution prevents the laser from being aimed exactly as desired. This influences the system's overall accuracy. A study of these two features led to a proposal to not modify the existing system at present.

Also undertaken was the design and construction of a Data Emulator. This device, which allowed testing data transactions with a PRIME computer, is described, and theory of operation briefly discussed. After testing and debugging this device, a full blown PRIME/Rover Interface was designed and built. The capabilities of this Interface are described and its operating principles briefly discussed.

PART 1

INTRODUCTION

1.1 History

In 1957 the space age was launched with the Sputnik. Ten years later R.P.I. became involved in the space exploration effort. In a project jointly funded by NASA and the Jet Propulsion Labs, R.P.I. began studying various problems associated with the unmanned exploration of Mars. In 1973 attention was directed toward designing and constructing a one-half scale prototype Mars Roving Vehicle (see Figure 1.1). This vehicle ('Rover') would carry an on-board laboratory and must be able to visit a number of sites.

R.P.I.'s research efforts are focused on the topic of obstacle detection and avoidance. In traversing from site to site, the Rover must be able to detect and avoid obstacles on an unknown terrain. One might guess that the vehicle could be radio controlled from earth. This is impractical because the round trip radio-communication time to Mars ranges from nine to 45 minutes. Instead of being directly controlled from earth, the vehicle would be an Autonomous Mars Roving Vehicle. The heading of the vehicle to a site of interest could be selected by earth-based researchers on the basis of pictures of the Martian terrain. A computer on board the Rover would select its path around obstacles as it made its way to that site.

By 1977 the prototype 'Rover' had been constructed. It featured an on-board hazard detection system, and was operated under the control of the Varian 620i minicomputer via a radio link.

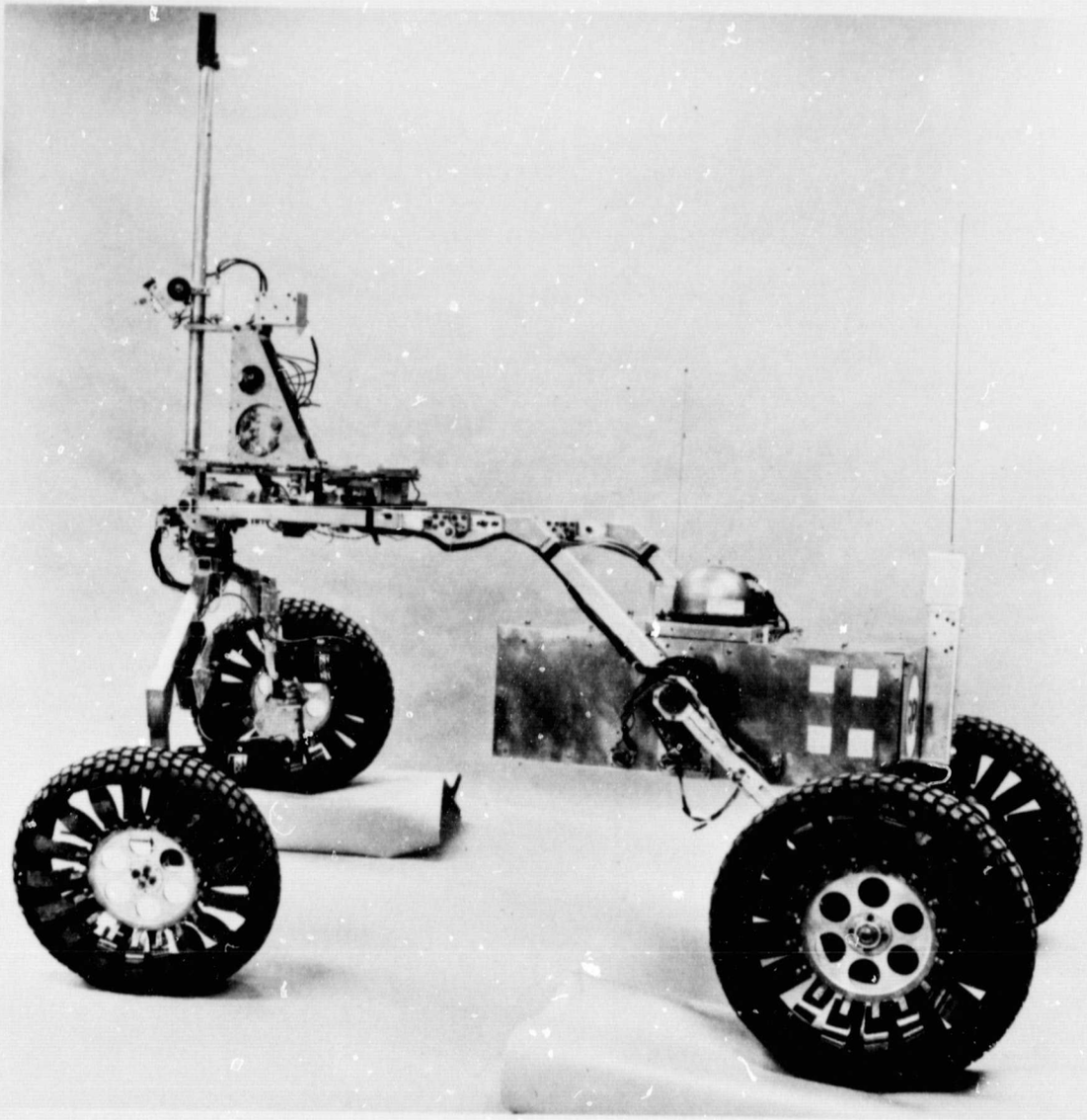

RENSSELAER AUTONOMOUS ROVING VEHICLE

Figure 1.1

Hazard detection was accomplished using a simple laser triangulation concept (see Figure 1.2). A laser was fired toward level ground at 15 evenly spaced azimuths over an arc of 140° (see Figure 1.3). A detector was also aligned and aimed such that on level ground the detectors would always receive reflected light from each laser shot (see Figure 1.4). Any unknown terrain which passed through the detector's cone of vision and reflected a laser shot into the detector was considered safe. A terrain-laser intersection point falling outside the detector's cone of vision would go undetected (see Figure 1.4). This terrain was considered unsafe. Using this concept one was able to distinguish between safe and unsafe terrain on the basis of returns from laser shots.

An advantage of this system over several alternate schemes is its ability to detect negative obstacles. A problem with it is that it tends to be a conservative system. By this we mean that it judges some terrain features to be 'unsafe', when in reality they are 'safe'. In laboratory and field testing this system performed remarkably well.

Beginning in 1977 work began on a higher level hazard detection system, known as the elevation scanning mast. This system fires 32 laser pulses at different elevations in each of 32 different azimuths, and detects returns using a 20-element linear photodiode array (see Figure 1.5). The elevation scanning mast produces about 1000 times more data than the previous system and is expected to be much less conservative.

The elevation scanning mast was completed in 1978. Since then attention has been concentrated on making a smooth transition

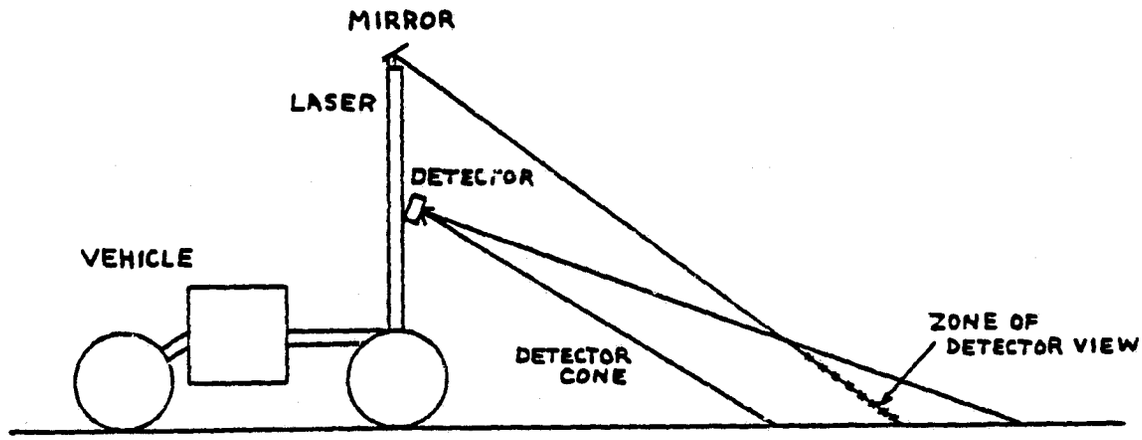

Figure 1.2. One Laser - One Detector System

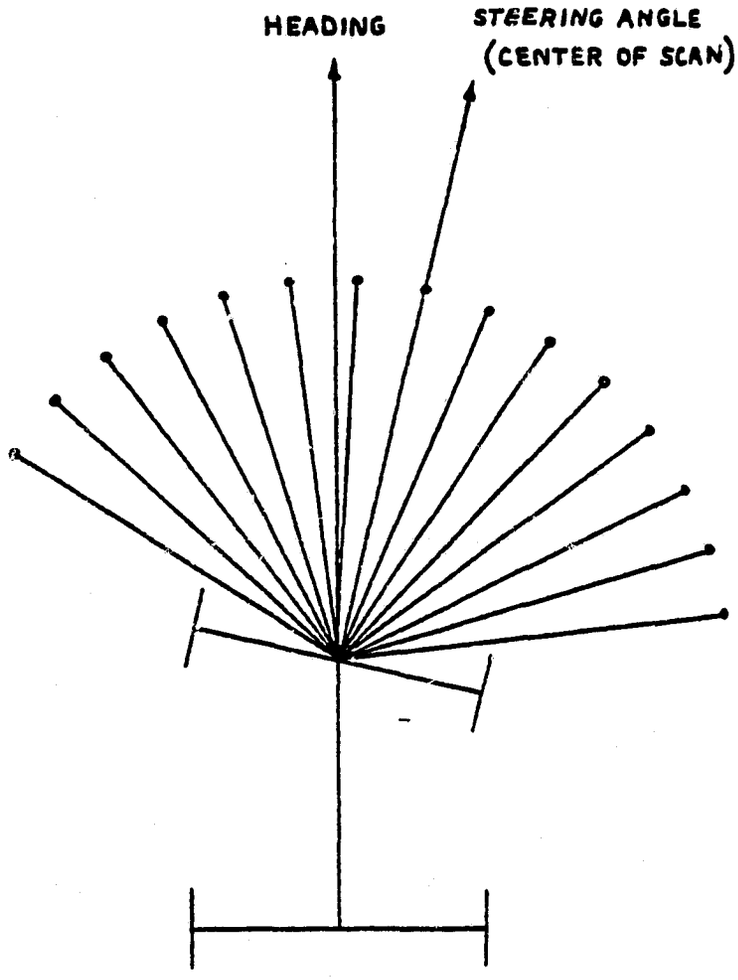

Figure 1.3. Laser Azimuths

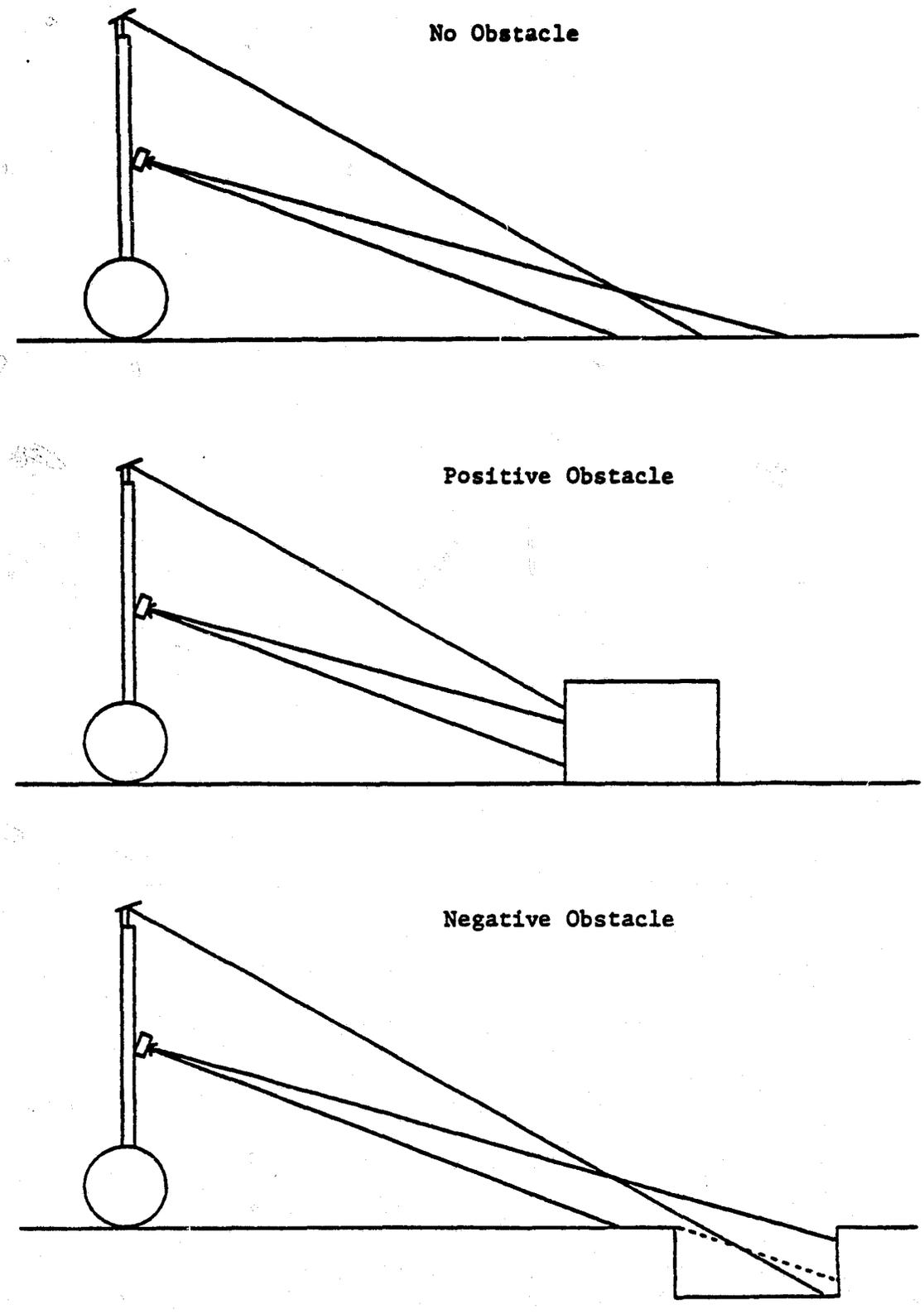

Figure 1.4. Laser Triangulation Concept

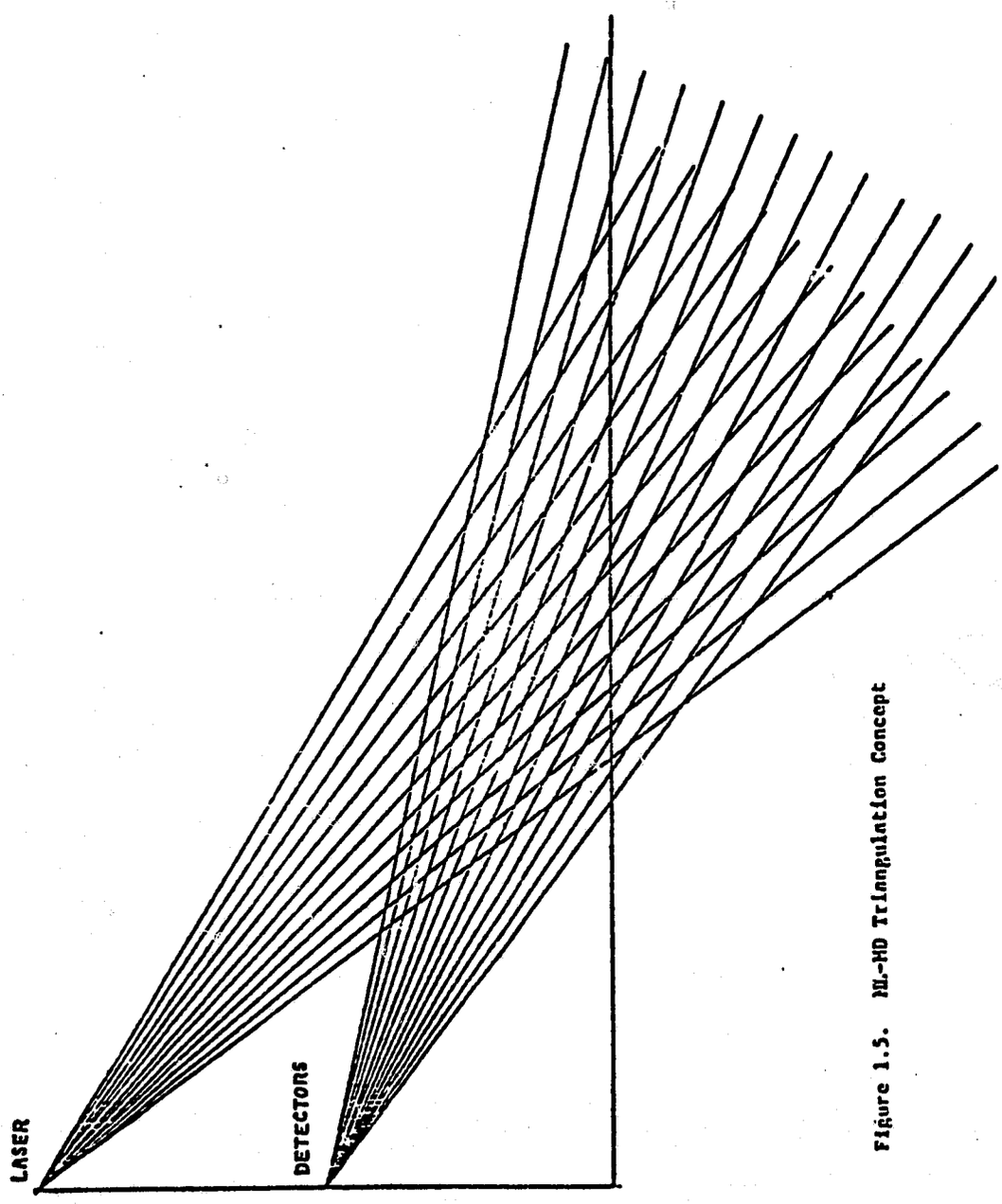

Figure 1.5. HL-HD Triangulation Concept

from using the old laser scanning mast to using the elevation scanning mast. This involved re-evaluating and redesigning several systems. This report deals with two topics. First, an evaluation of techniques for upgrading the elevation scanning mast. Second, the justification for, and design of, a new computer/Rover Interface.

1.2 Introduction to Laser Optics Appraisal

In 1978 Troiani developed a multi-laser, multi-detector (ML/MD) hazard detection concept. This concept requires that the laser be aimed at the center of each detector field (see Figure 1.6). The result is a quasi-linearized array that enables the inference of obstacle heights and slopes.

Based on computer simulations Troiani found that the ML/MD concept required a certain degree of resolution in order to be useful. By useful, we are here referring to a particular system's degree of conservatism. If a given system's performance is such that it operates no less conservatively than the single laser-single detector scheme, then it would not be useful. Our objective here is not to take a photograph of the terrain, but to accurately detect and avoid obstacles.

Troiani's simulations reveal that a 15 laser by 20 detector system with a 2°/detector field of view was marginally 'useful'. A 25 laser by 30 detector system with 1.33°/detector field of view proved to be better. A 32 laser by 40 detector system looking at 40° (1.0°/detector), understandably, yielded even better results.

The elevation scanning mast is a 32 laser by 20 detector system looking at 32° (1.55°/detector). The position of the mirror

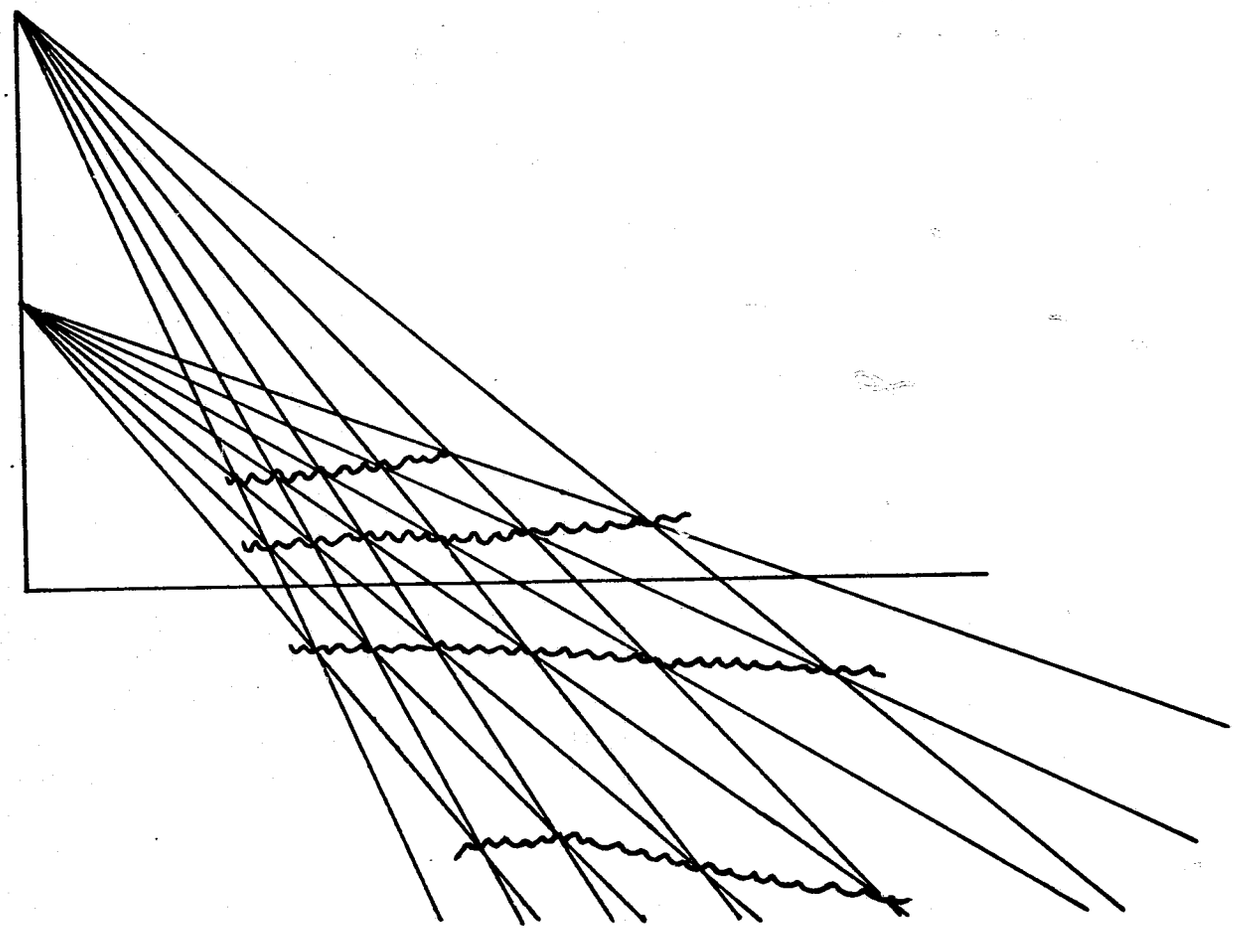

Figure 1.6. Troiani ML-MD Triangulation Concept

which directs the 32 laser pulses is monitored by a shaft encoder having a resolution of .35°.

Having less than 40 detectors will result in a resolution less than indicated by Troiani's simulations using a 32 laser by 40 detector scheme. The shaft encoder's finite resolution will create an accuracy problem. A study of the first consideration led to a proposal for increasing the resolution of the elevation scanning mast without modifying hardware. A study of the second consideration led to the conclusion that nothing should be done about the shaft encoder's .35 resolution at present.

1.3 The Data Emulator and PRIME/Rover Interface

In December 1978 a decision was made to begin using the Image Processing Laboratory's (IPL's) PRIME 500 computer as the brain for the Mars Rover. Up until then a VARIAN 620i had served this purpose. The decision was made for several reasons. First, the PRIME computer would allow the software group to write their artificial intelligence algorithms in FORTRAN. Use of the VARIAN required extensive knowledge of assembly language. Assembler is cumbersome and hard to debug. This switch would simplify the programmer's task. Second, by moving to the new machine one would be able to process data faster. Higher speed was considered a necessity because of the vast increase in data available from the elevation scanning mast. The old mast produced one 16 bit word per sweep (see Figure 1.7). The elevation scanning mast produces 1024 words per scan. This data must be processed quickly, decisions made, and commands sent back to the Rover

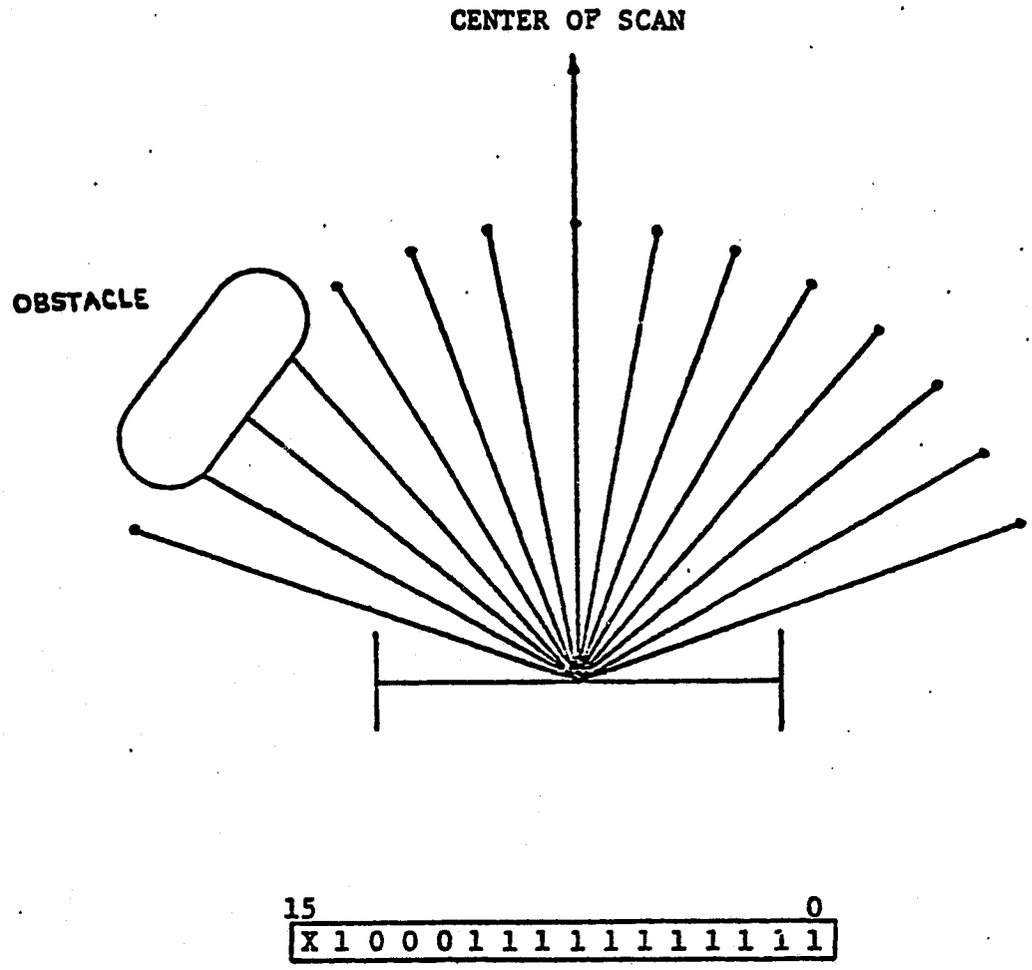

Figure 1.7. Laser Data Word

in order to avert crisis situations.

After deciding to move software operations to the IPL's PRIME computer, the next question was how to interface to this machine. Using an AMLC-type interface did not allow high enough data rates. These commonly allow 8.6 kbaud with the possibility of going to 19.2 kbaud. Our laser data rates were calculated to be approximately 66.9 kbaud. It was found that PRIME manufactures a General Purpose Interface Board (GPIB) that allows 16 bit word transfers with rates as high as 1.25×10^6 words per sec. This would clearly meet our needs.

As a first step toward building a PRIME/Rover interface it was decided to construct a Data Emulator. This was to be a multifunction device capable of providing multiple word transfers in any DMX mode (DMX is a generic term which includes specific processes such as DMA, DMC, DMT, DMQ) and Interrupt Requests in the absence of real data from the Rover. In addition to this, it must keep track of Interrupt Processing time. This would give us some indication of how heavily we were loading the computer.

The purpose of the Data Emulator was fourfold. First, it would provide a test bed for finding out as much as possible about the protocol required to interface to the PRIME through the GPIB. Second, it would provide information on how heavily our Interrupt Service Routine (ISR) was loading the whole system. This information was made available by keeping track of Interrupt Processing time. Thirdly, by using data flows and interrupts from the Data Emulator, one would be able to debug software that was under development. Finally, as the PRIME/Rover Interface was being built, the Data Emulator could provide

debugging aids without requiring an operating data link from the Rover.

After designing, building and debugging the Data Emulator, the next step of designing, building and debugging the complete PRIME/Rover Interface was to be a natural, simple step forward. The following documentation describes the Data Emulator and the PRIME/Rover Interface as designed by the author.

PART 2

LASER OPTICS APPRAISAL

2.1 The Problem

Two concerns confronting any scheme for detecting and avoiding obstacles are those of accuracy and resolution. It is not enough to be able to detect an object, one must be able to determine its position and describe its extent. This information gives the entity seeking to avoid obstables a criterion on which to make decisions. The accuracy and resolution with which one is able to do this will influence the system's conservativeness. It does little good to have one of these features without the other. For example, to know the position of an obstacle is meaningless if one's edge detecting resolution is so poor that one cannot describe the obstacle's extent. Likewise, it doesn't help to have high edge detecting resolution if some inherent error in the sensing device gives one a poor idea where the obstacle is located.

2.2 Resolution

For a given obstacle pattern, it has been found that the motion of an obstacle detecting entity becomes less constrained as the resolution of the entity's sensory information increases. Simulations done using Troiani's concept demonstrated that as the number of lasers and detectors increased, the resolution increased. He found that a 32 laser by 40 detector system, looking at 40° (1° per detector) produced excellent results. Excellent in that the simulated vehicle could, with low ambiguity, differentiate between obstacle and non-

obstacle terrain.

The elevation scanning mast has 32 laser per azimuth capability, but is equipped with only 20 detectors, each with a field of view of 1.55°. The question facing us is, how could this system be upgraded to meet Troiani's specifications. There are several approaches:

1.) Use a second 20 element array identical to the one now in use. By concatenating the fields of view, one could meet Troiani's specifications.

2.) Look for arrays with more elements. If a 40 element linear photodiode array became available it could be used to replace the 20 element array now in use. Alternatively one could use "Reticon's" 1024 element charge coupled device photodiode array.

3.) Make the 20 element array look like a 38 element array.

The first approach is being investigated by Jim Odenthal. Using two 20 element arrays would be compatible with our system. One problem with this approach would be maintaining the proper alignment of the two detectors. This problem would be aggravated when the vehicle is tested on real, that is bumpy, terrain.

At present, the second approach is not being actively pursued. Forty element linear photodiode arrays seem to be unavailable. In addition to this, early experiments with the 'Reticon' 1024 element device indicate that it lacks sufficient sensitivity. Until new devices become commercially available, this approach does not look feasible. New, higher resolution devices should be investigated as they come on the market.

In the Fall semester of 1978 I was given responsibility

for investigating the third approach. There were two different techniques for 'tricking' a 20 element array into acting like a 38 element array. One involved using a highly collimated laser beam and is known as the Laser Overlay Concept (LOC). The other involved using a divergent laser beam and is called the Voting Detector Concept (VDC).

The Laser Overlay Concept requires that Troiani's Laser-Detector intersection pattern (Figure 2.1) be modified. The modified version is illustrated in Figure 2.2. As indicated by Troiani's plan, a series of laser pulses would be aimed at the mid-points of each detector field. These are illustrated in Figure 2.2 by 1A, 2A, 3A, etc. Interleaved between these lasers would be laser shots aimed at the intersections of level ground with the edges of each detector field. These are labeled 1B, 2B, 3B, etc. The laser firing sequence would be 1A, 1B, 2A, 2B, 3A, 3B..... Now, how does this increase one's resolution?

Look at the terrain in the illustration. Detector One will see Laser 1A. Detector Two will see Laser 1B and Laser 2A. Detector Three will see Laser 2B only. This has been tabulated below.

Laser	Detector
1A	1
1B	2
2A	2
2B	3

By comparing detector responses to the corresponding 'A' and 'B' lasers, one's resolution can effectively be doubled. For example,

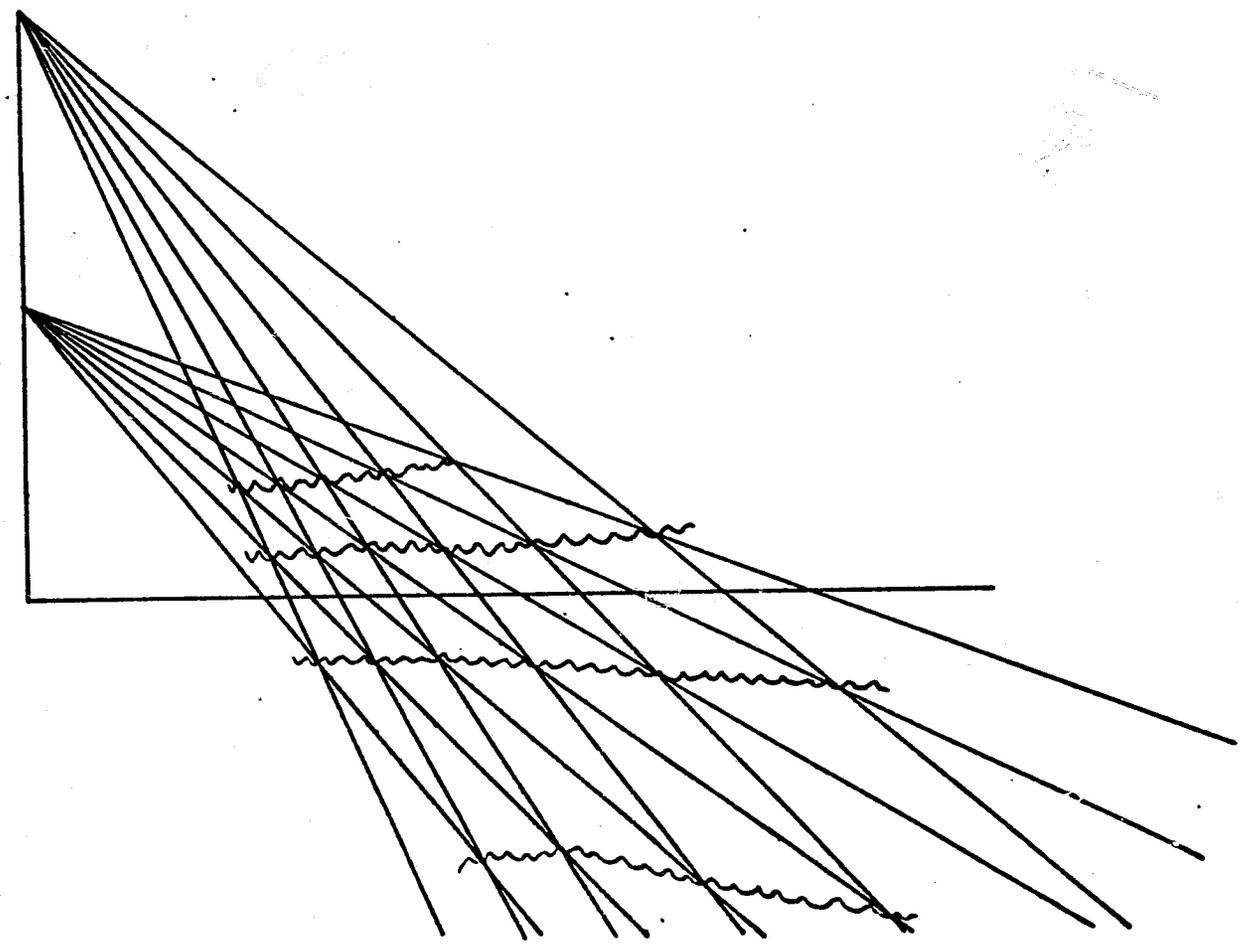

Figure 2.1. Troiani ML-MD Triangulation Concept

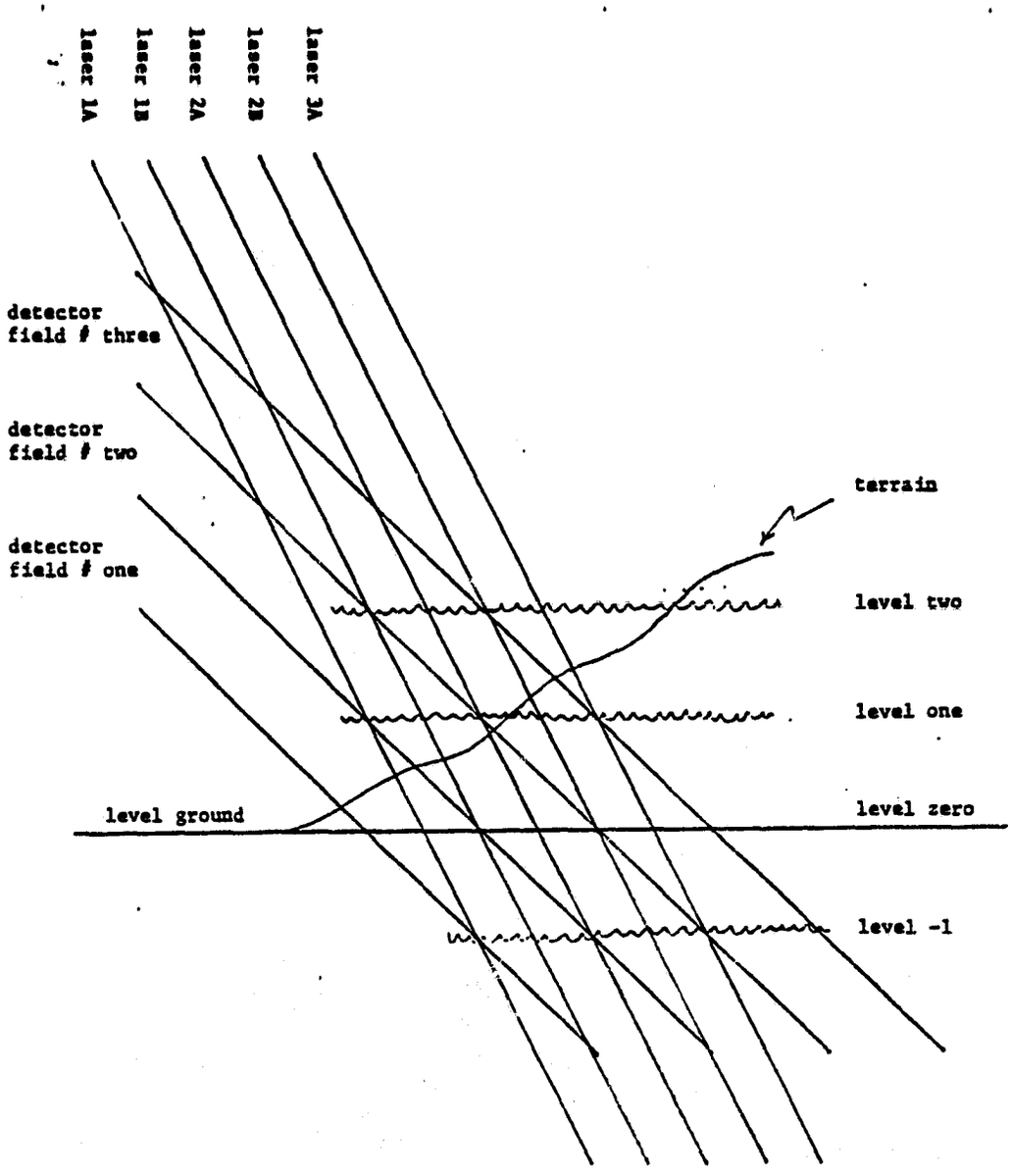

Figure 2.2. Laser Overlay Concept

Detector One 'sees' Laser 1A. Detector Two 'sees' Laser 1B. Now, assuming the terrain's height does not change radically between laser shots (this is considered a reasonable assumption because the lateral displacement between laser shots is approximately 5 cm.) one can infer that it lies between level 0 and level 1. The logic involved is described as follows.

'If Detector 1 responds to Laser 1A and Detector 2 responds to Laser 1B, then terrain is located in Quantum Level +1. If Detector 1 responds to Laser 1A and Detector 1 responds to Laser 1B, then terrain lies within Quantum Level -1. Thus, the general logic compares the detector responses to Laser nA and Laser nB to assign the terrain location.'(1)

Locally steep gradients, such as edges of rocks, could invalidate our assumption that the terrain's height does not change radically between laser shots. These changes would only be important if they were severe enough to constitute a hazard. In this case, subsequent laser shots will pick out the hazard.

Realizing the Laser Overlay Concept physically, involves creating a highly collimated laser beam. This is the chief drawback of this scheme. Designing the optics to create a well collimated beam (beam exit diameter, from the collimation optics, on the order of 4 mm) from a laser diode stack, is no trivial task. With commercial units expense becomes the dominant consideration. In addition to this, any scheme used to collimate the laser will attenuate the signal. This will reduce the effective range of the elevation scanning mast. Another drawback has to do with the characteristics

of the detector array now in use. The detector array is a 20 element linear photodiode array. Between each detector is a deadband of .05 mm. At a distance of two meters from the detector, taking into account the detector optics, one finds that there is a 3 mm deadband between detector fields. A highly collimated laser could be lost in such a gap.

The second technique for resolution enhancement known as the Voting Detector Concept involves using a diffuse laser beam, aimed in the manner Troiani specified. This technique is illustrated in Figure 2.3. An explanation of how the resolution is enhanced is given below. When Laser 1 fires, only detector 1 'sees' it. When Laser 2 fires, detectors 2 and 3 respond. If the terrain is 'seen' by only one detector, then one knows that it must be in the zone where the laser falls completely within a single detector field. In Figure 2.3, height level 0 is such an area. If two detectors 'see' a given laser pulse, then the terrain must lie somewhere in the zone where the laser is crossing from one detector field to another. In Figure 2.3, height level 1 is such an area. Figure 2.4 shows how the size of height level 0 and height level 1 change as the laser beam becomes increasingly collimated. One can see that height level 0 becomes larger and height level 1 shrinks. In the limit, as the collimation increases to the point where the laser beam is a line, height level 1 becomes a point and height level 0 becomes as large as could be realized in Troiani's unmodified scheme. If instead of increasing the laser's collimation, we decrease it below that shown in Figure 2.3, one finds that height level 0 shrinks and height

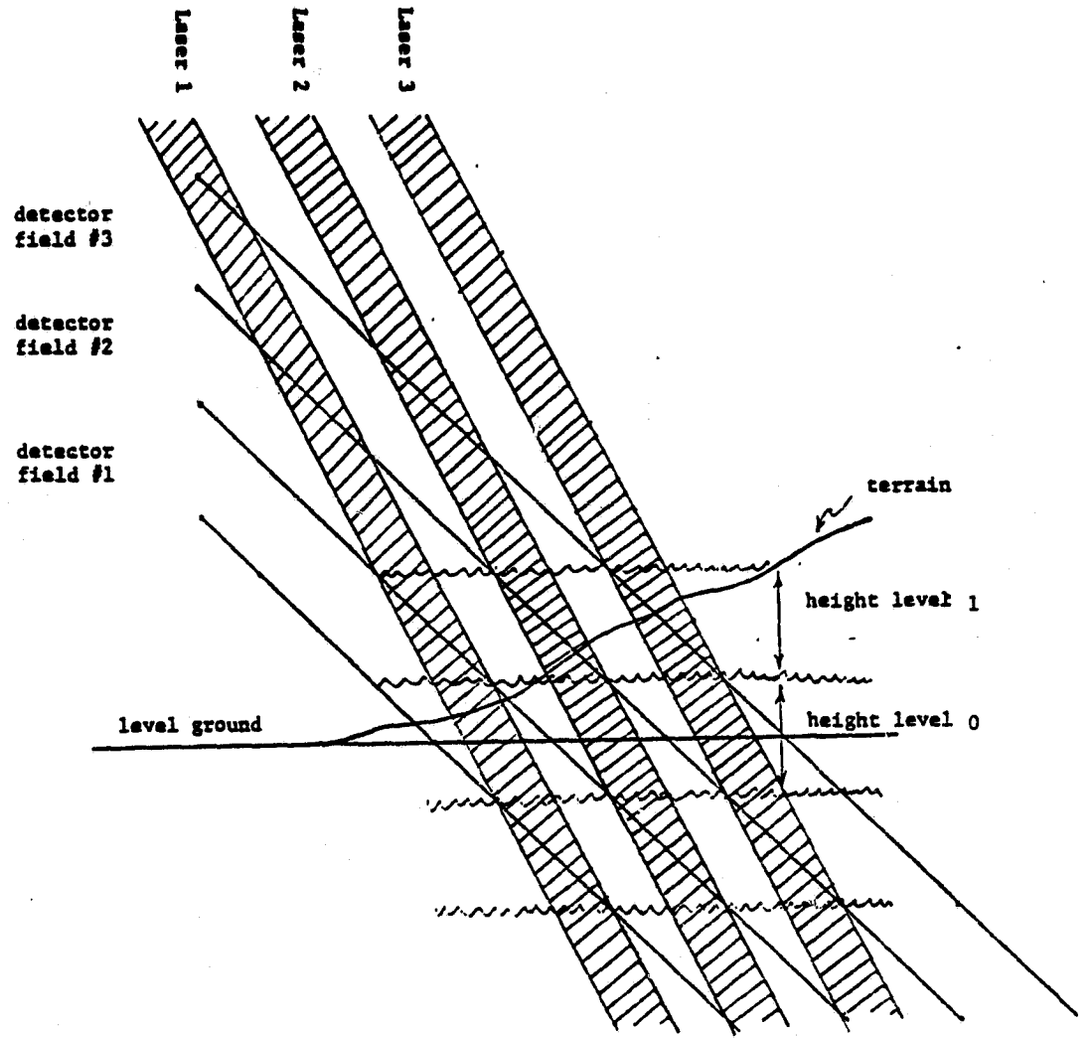

Figure 2.3. Voting Detector Concept

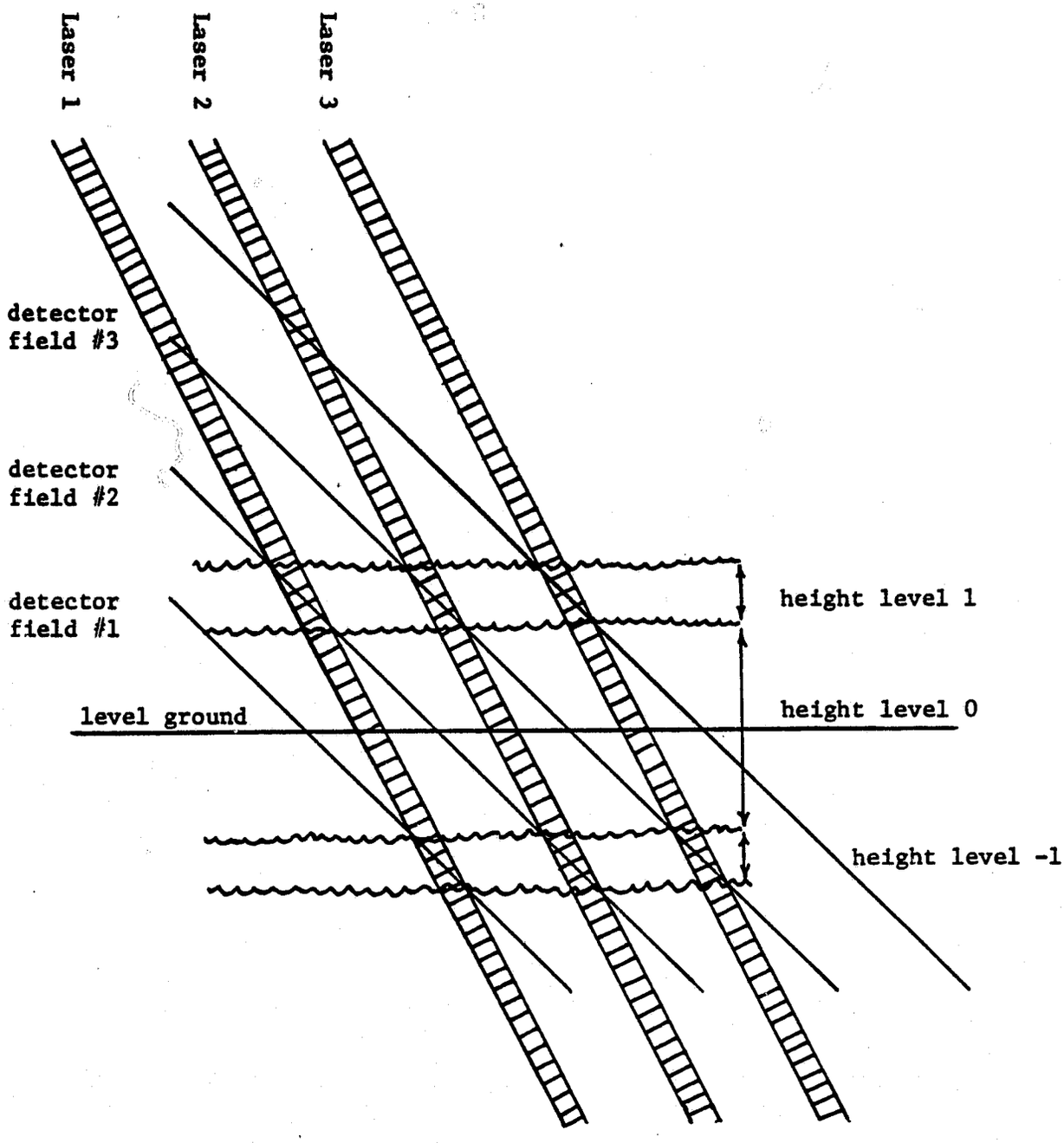

Figure 2.4. Voting Detector, Non-Optimal Laser Width

level 1 expands. The optimum collimation is when the laser beam covers one-half of a given detector field. In this case height levels are roughly equal, and are half as large as the corresponding levels in Troiani's scheme. It is because of this that the resolution throughout the Laser-Detector field has doubled.

The Voting Detector Concept has a number of advantages over the Laser Overlay Concept. First, steep gradients are not a consideration in determining the terrain position. Second, it does not require sophisticated optics. A single aspheric lens can be used to collimate the laser spot to a diameter less than one-half a given detector's field of view on level ground. Then by defocusing the detector lens one could adjust the laser beam's diameter as seen by the detectors to the desired value. Third, this scheme does not require that the laser pulse rate be increased over its present value. In addition to this, by not attempting sophisticated laser collimation one's power output is higher. Thus the range of the elevation scanning mast will not be unnecessarily decreased. Finally, with a broad beam, losing the laser in a deadband would be less likely.

2.3 Accuracy

As mentioned earlier, the problem of providing adequate accuracy is also important when devising obstacle detection sehemes. In the new elevation scanning mast the question of providing adequate accuracy becomes an important consideration when studying the influence of the mirror shaft encoder's finite resolution on data interpretation.

The mirror shaft encoder on the elevation scanning mast has a resolution of .35 degrees. Implementing Troiani's concept involves aiming the laser directly at the midpoint of a given detector field on level ground. Because of the shaft encoder's finite resolution this is impossible. One must be satisfied with aiming one's laser to within .175 degrees of the correct angle. How does this influence one's accuracy? Figure 2.5 shows the theoretical and actual Laser-Detector intersection points for a hypothetical system. Based on the detector response for the situation illustrated, one would predict the terrain to lie between points A and B. In actuality the terrain lies between points C and D. It is apparent that if one predicts the terrain as lying in a certain band based on the theoretical results, one could be wrong. Depending on the extent of this effect, one may or may not have a problem.

Computer simulations done in Fall 1978, ignoring the mirror shaft encoder's .35 degree resolution, produced the results tabulated in Table 2.1. Simulations done taking into account the shaft encoder's finite resolutions are tabulated in Table 2.2. The results in these tables are illustrated in Figure 2.6. Here one sees that the .35 degree resolution produces only a 3 cm perturbation over 2 meters. When viewed in this way the perturbation is relatively minor. When viewed as a percentage of the whole level it becomes more significant. The Figure reveals that the actual Laser-Detector intersection points vary approximately $\pm$ 1.5 centimeters over a quantum level which is approximately 10 centimeters wide. The error viewed in this way is approximately $\pm$ 15%.

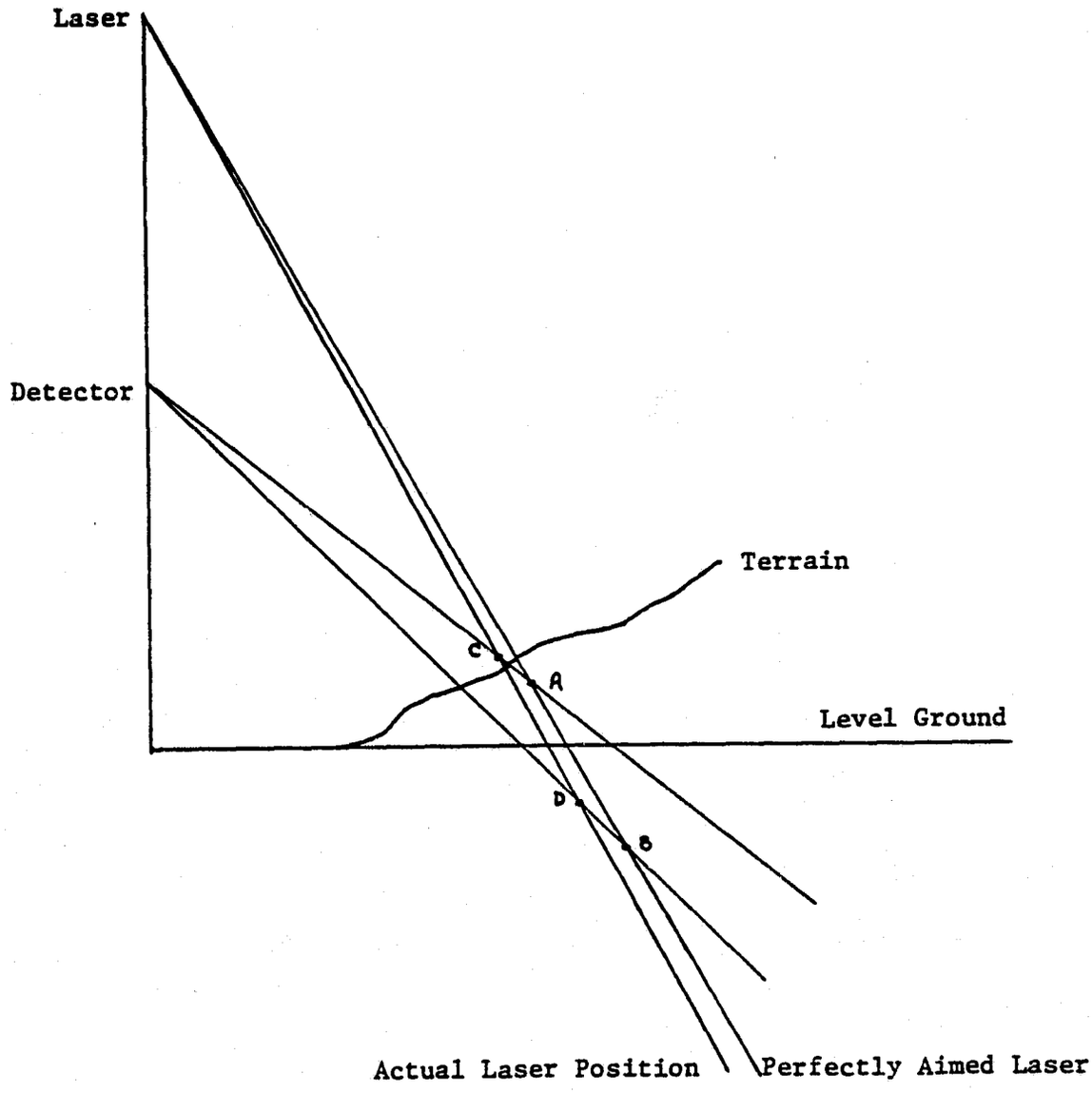

Figure 2.5. Hypothetical Laser-Detector Intersection Points

β deg.	X_2 cm	Y_2 cm	X_5 cm	X_5 cm
21.80°	82.3	-5.7	78.0	5.1
22.88°	86.8	-5.6	82.3	5.0
23.98°	91.4	-5.6	86.7	5.0
25.12°	96.4	-5.5	91.4	5.0
26.30°	101.6	-5.5	96.4	5.0
27.51°	107.0	-5.5	101.5	5.0
28.76°	112.8	-5.5	107.0	5.0
30.05°	118.9	-5.6	112.8	5.0
31.39°	125.5	-5.6	118.9	5.1
32.77°	132.4	-5.7	125.5	5.1
34.21°	139.9	-5.8	132.4	5.2
35.70°	147.9	-5.9	139.9	5.3
37.24°	156.6	-6.0	147.9	5.4
38.85°	166.1	-6.2	156.6	5.5
40.52°	176.4	-6.4	166.1	5.7
42.25°	187.7	-6.6	176.4	5.8
44.05°	200.1	-6.9	187.7	6.0
45.93°	214.0	-7.1	200.1	6.3
47.88°	229.5	-7.5	214.0	6.5
49.91°	247.0	-7.9	229.5	6.8

Table 2.1 Laser-Detector intersection points ignoring encoder's finite resolution.

β^* deg.	X_2^* cm	Y_2^* cm	X_5^* cm	Y_5^* cm
21.70	81.4	-4.6	77.2	6.0
22.75	85.7	-4.3	81.3	6.2
24.15	92.9	-7.3	88.1	3.5
25.20	97.1	-6.3	92.1	4.3
26.25	101.1	-5.1	96.0	5.3
27.65	108.4	-6.9	102.8	3.8
28.70	112.3	-5.0	106.5	5.4
30.10	119.4	-6.0	113.2	4.6
31.50	126.6	-6.6	120.0	4.2
32.90	133.8	-6.8	126.7	4.2
34.30	140.9	-6.6	133.3	4.6
35.70	148.0	-5.9	139.9	5.3
37.10	155.0	-4.9	146.5	6.3
38.85	166.1	-6.2	156.7	5.5
40.60	177.5	-7.0	167.0	5.1
42.35	189.0	-7.4	177.6	5.2
44.10	200.8	-7.2	188.3	5.7
45.85	212.7	-6.5	199.1	6.8
47.95	230.6	-8.0	215.0	6.1
50.05	249.5	-9.0	231.7	5.9

Table 2.2 Laser-Detector intersection points including encoder's finite resolution.

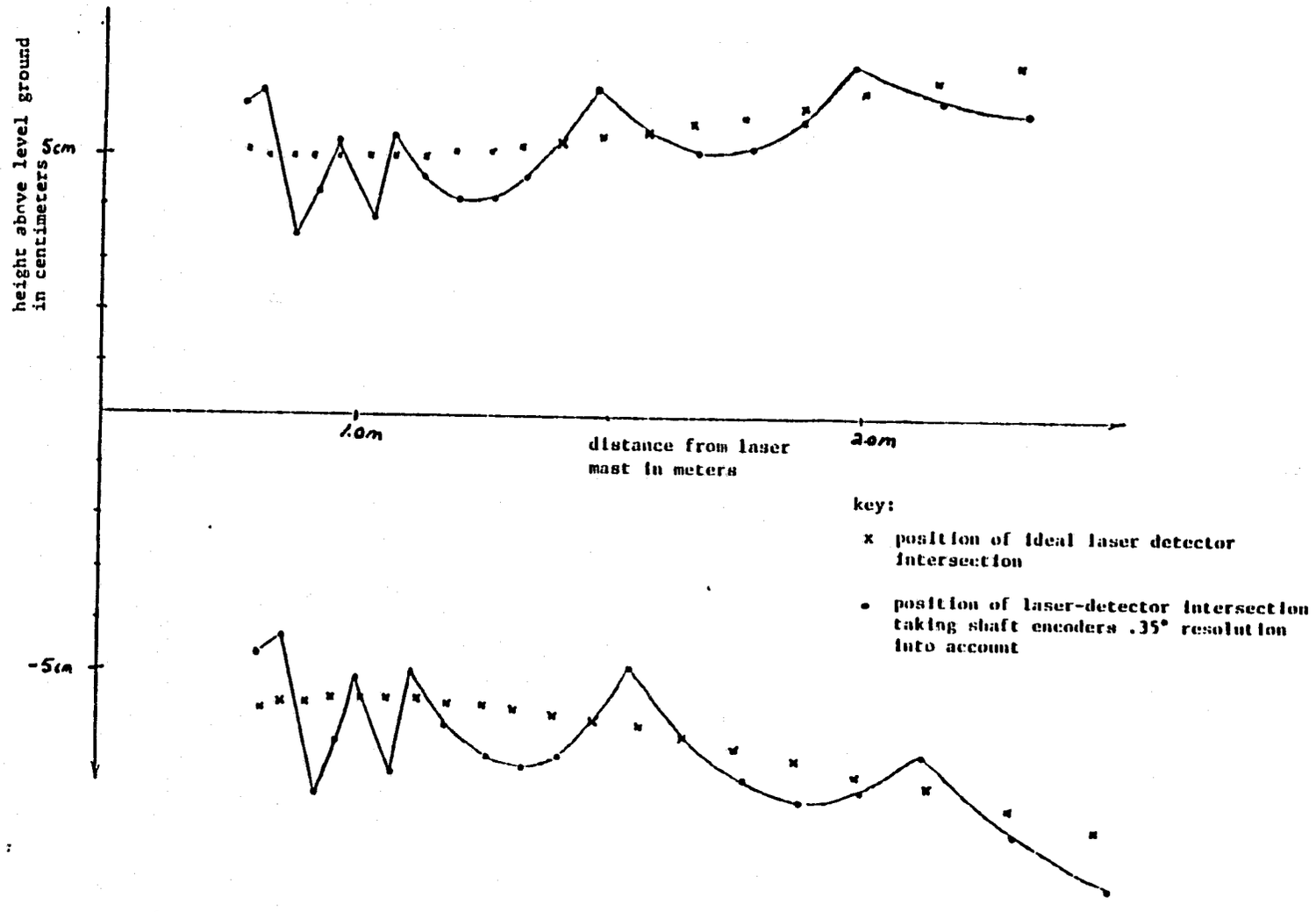

Figure 2.6. Upper and Lower Endpoints for Level Ground Quantum Level for a 20 x 20 System.

Computer simulations were also done using the Voting Detector Concept ignoring and taking into account the .35 degree encoder resolution. The results are tabulated in Tables 2.3 and 2.4, and illustrated in Figures 2.7 and 2.8. In this case the perturbation over 2 meters is still roughly 3 centimeters. The percentage error for a given quantum level jumps to approximately $\pm$ 30% though because the quantum levels are half as large.

2.4 Conclusion

In view of the several advantages that the Voting Detector Concept has over the Laser Overlay Concept it is my recommendation that it be implemented for resolution enhancement. Despite its many advantages one should not get the Utopian view that the VDC eliminates all one's problems. The existence of a deadband and the detector response thresholds ruin the beautiful picture. One must still answer questions such as: How much of the laser must fall within a given detector field before it is 'seen'? and, How big must the laser beam be to bridge the deadband and still be 'seen' by two detectors? These questions must be answered experimentally before the VDC's viability can be fully ascertained.

The problem of improving the mirror shaft encoder's finite resolution was studied in the Fall semester of 1978. The encoder may be electronically or mechanically modified to improve its resolution. It is my opinion that such modifications are at present unnecessary. The inaccuracies inherent in the system when it operates on a real terrain will be greater than those due to the shaft encoder's finite

β deg.	X_1 cm	Y_1 cm	X_3 cm	Y_3 cm
21.80	80.0	-2.8	84.6	-8.6
22.88	84.5	-2.8	89.1	-8.5
23.98	89.1	-2.9	93.8	-8.3
25.12	94.0	-3.0	98.8	-8.2
26.30	99.2	-3.0	104.0	-8.1
27.51	104.6	-3.1	109.5	-8.0
28.76	110.3	-3.2	115.4	-8.0
30.05	116.4	-3.3	121.6	-7.9
31.39	122.8	-3.4	128.2	-7.9
32.77	129.7	-3.5	135.2	-8.0
34.21	137.1	-3.7	142.8	-8.0
35.70	145.0	-3.8	151.0	-8.1
37.24	153.6	-4.0	159.8	-8.2
38.85	162.9	-4.2	169.4	-8.3
40.52	173.0	-4.4	179.8	-8.5
42.25	184.1	-4.6	191.3	-8.7
44.05	196.4	-4.8	204.0	-8.9
45.93	209.9	-5.1	218.2	-9.2
47.88	225.1	-5.4	234.02	-9.6
49.91	242.2	-5.8	251.9	-10.0

Table 2.3a Laser-Detector intersection points for Voting Detector Concept ignoring encoder's finite resolution.

β deg.	X_4 cm	Y_4 cm	X_6 cm	Y_6 cm
21.80	76.0	7.5	80.0	2.6
22.88	80.2	7.4	84.4	2.6
23.98	84.7	7.3	88.9	2.7
25.12	89.3	7.2	93.6	2.7
26.30	94.2	7.1	98.6	2.8
27.51	99.3	7.0	103.8	2.9
28.76	104.8	7.0	109.3	2.9
30.05	110.5	7.0	115.2	3.0
31.39	116.5	7.0	121.4	3.1
32.77	123.0	7.0	128.0	3.2
34.21	129.9	7.0	135.0	3.3
35.70	137.3	7.1	142.6	3.5
37.24	145.2	7.1	150.7	3.6
38.85	153.8	7.2	159.6	3.8
40.52	163.1	7.4	169.1	3.9
42.25	173.2	7.5	179.6	4.1
44.05	184.3	7.7	191.1	4.3
45.93	196.6	7.9	203.8	4.5
47.88	210.2	8.2	217.9	4.8
49.91	225.4	8.5	233.7	5.1

Table 2.3b Continuation of Table 2.3a.

β^* deg.	X_1^* cm	Y_1^* cm	X_3^* cm	Y_3^* cm
21.70	79.2	-1.7	83.7	-7.5
22.75	83.4	-1.6	88.0	-7.1
24.15	90.6	-4.6	95.4	-10.1
25.20	94.7	-3.7	99.5	-9.0
26.25	98.8	-2.6	103.6	-7.6
27.65	105.9	-4.4	110.9	-9.4
28.70	109.8	-2.7	114.8	-7.4
30.10	116.8	-3.7	122.1	-8.4
31.50	123.9	-4.4	129.4	-8.9
32.90	131.0	-4.6	136.6	-9.1
34.30	138.1	-4.4	143.8	-8.8
35.70	145.0	-3.8	151.0	-8.1
37.10	152.0	-2.9	158.1	-7.0
38.85	162.9	-4.2	169.4	-8.3
40.60	174.1	-5.0	180.9	-9.1
42.35	185.4	-5.3	192.7	-9.5
44.10	197.0	-5.2	204.7	-9.3
45.85	208.7	-4.5	216.9	-8.6
47.95	226.2	-6.0	235.2	-10.1
50.05	244.7	-6.9	254.5	-11.2

Table 2.4a Laser-Detector intersection points for Voting Detector Concept including encoder's finite resolution.

β^* deg.	X_4^* cm	Y_4^* cm	X_6^* cm	Y_6^* cm
21.70	75.2	8.5	79.2	3.5
22.75	79.3	8.5	83.3	3.8
24.15	86.0	5.9	90.3	1.2
25.20	89.9	6.5	94.3	2.0
26.25	93.8	7.5	98.2	3.2
27.65	100.5	5.9	105.1	1.7
28.70	104.3	7.4	108.8	3.4
30.10	110.9	6.6	115.6	2.6
31.50	117.6	6.2	122.4	2.3
32.90	124.2	6.1	129.2	2.3
34.30	130.8	6.4	135.9	2.7
35.70	137.3	7.0	142.6	3.4
37.10	143.8	8.1	149.2	4.6
38.85	153.8	7.2	159.6	3.7
40.60	164.0	6.8	170.1	3.4
42.35	174.4	6.9	180.8	3.5
44.10	184.9	7.4	191.7	4.0
45.85	195.5	8.4	202.7	5.1
47.95	211.2	7.8	218.9	4.4
50.05	227.5	7.6	236.0	4.2

Table 2.4b Continuation of Table 2.4a.

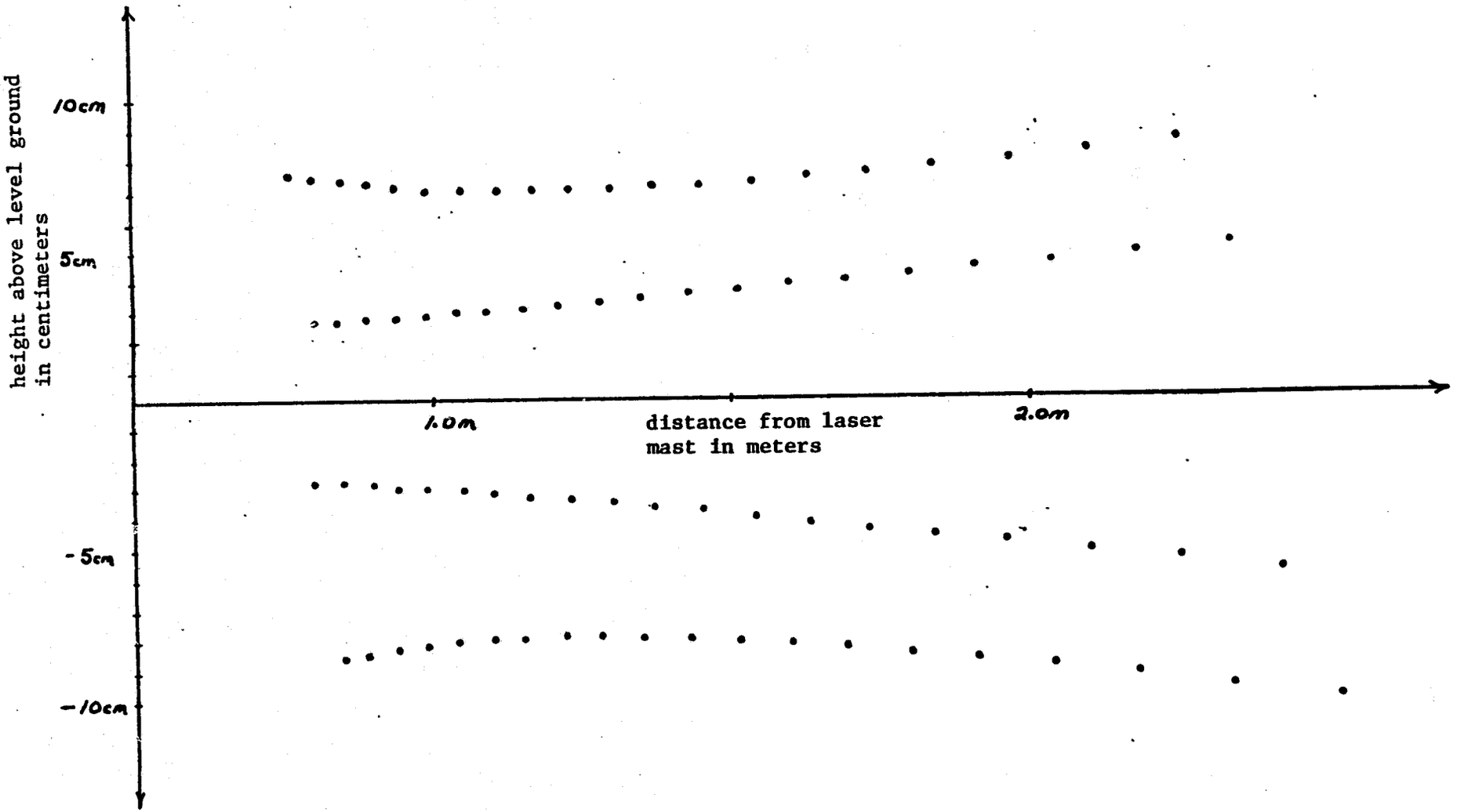

Figure 2.7. Laser-Detector Intersection Points for Voting Detector Concept Ignoring Encoder's Finite Resolution

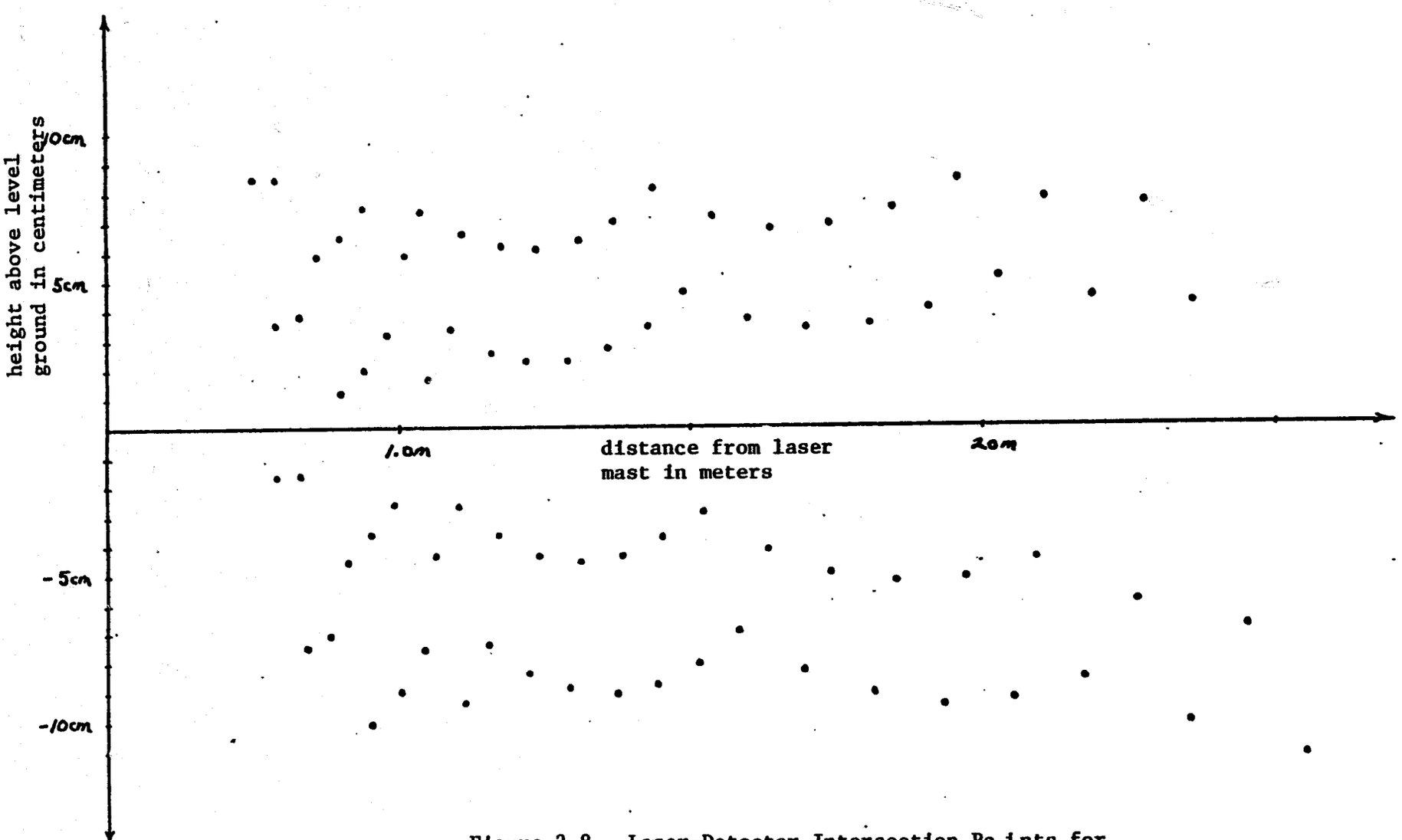

Figure 2.8. Laser-Detector Intersection Points for Voting Detector Concept Including Encoder's Finite Resolution

resolution. It would therefore seem wise to do some field testing prior to making any modifications to the present system.

PART 3

THE DATA EMULATOR AND PRIME/ROVER INTERFACE

3.1 The Data Emulator

The Data Emulator was a test circuit designed as a first step toward building a PRIME/Rover Interface. As a test circuit its purpose was fourfold: 1) It should serve as a test bed for finding out as much as possible about the protocol required to interface to the PRIME computer; 2) It should provide information on how heavily our interface software (Interrupt Service Routine) loads the computer; 3) It should be an aid to debugging software; 4) It should be an aid to debugging the PRIME/Rover Interface hardware as it is being built.

To fulfill the design specifications above, the Data Emulator had to be versatile and capable of imitating the proposed interface, at lease on a primitive level. A few of the Data Emulator's capabilities are listed below.

1.) It was capable of transferring two different words in any DMX mode. Data words used were switch selectable. Changing from one DMX mode to another required some minor hardware modifications. Multiple word transfers could be done by altering hardware more significantly.

2.) It provided Interrupt Requests in the absence of any real data from the Rover. These came in between the data words transferred.

3.) It contained a 'stopwatch' to clock how much time the Interrupt Service Routine (ISR) consumed.

Construction of the Data Emulator was complete by early

March 1979. After this it entered a long period of debugging that extended over several months. Simple problems with the design, such as reversed address lines, were located early. Other problems were solved by talking to PRIME by phone.

After eliminating the simple problems the Data Emulator began showing signs of life, but its operation was erratic. It would do anywhere from one to several thousand interrupts and then unexplainably the computer would undergo a syscrash. This problem went undiagnosed for several months. Finally in early October 1979, with the help of Michael Potmesil, it was discovered that the address line tri-states, in the portion of the GPIB constructed by PRIME, were flakey. When the Data Emulator was the only device using the bus, it operated flawlessly. When operated in conditions where time constraints existed, such as when the disk was using the bus heavily, the system would fail. Apparently the tri-states were putting bad address information on the bus. After changing tri-states the Data Emulator began to function perfectly. After testing the Data Emulator thoroughly, energy was directed toward designing and constructing the PRIME/Rover Interface.

3.2 Operating Principles

Figure 3.1 shows the relationship of the Data Emulator to the whole system. Figure 3.2 is a block diagram of the Data Emulator. Within this figure is a counter whose outputs are labeled α, β and γ. It provides the control timing for the Data Emulator. Figure 3.3 shows the outputs from the counter, as would be seen on an oscilloscope, were the counter not connected to other circuitry. As can be seen, gamma is

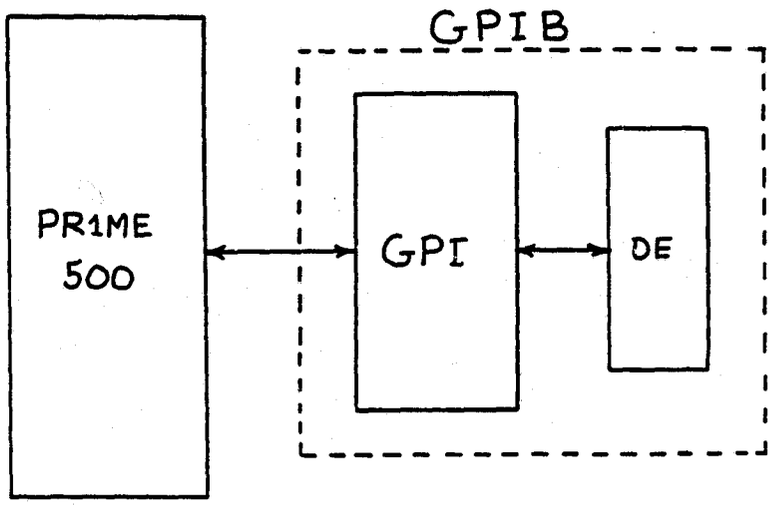

Figure 3.1. PRIME/Data Emulator System Configuration

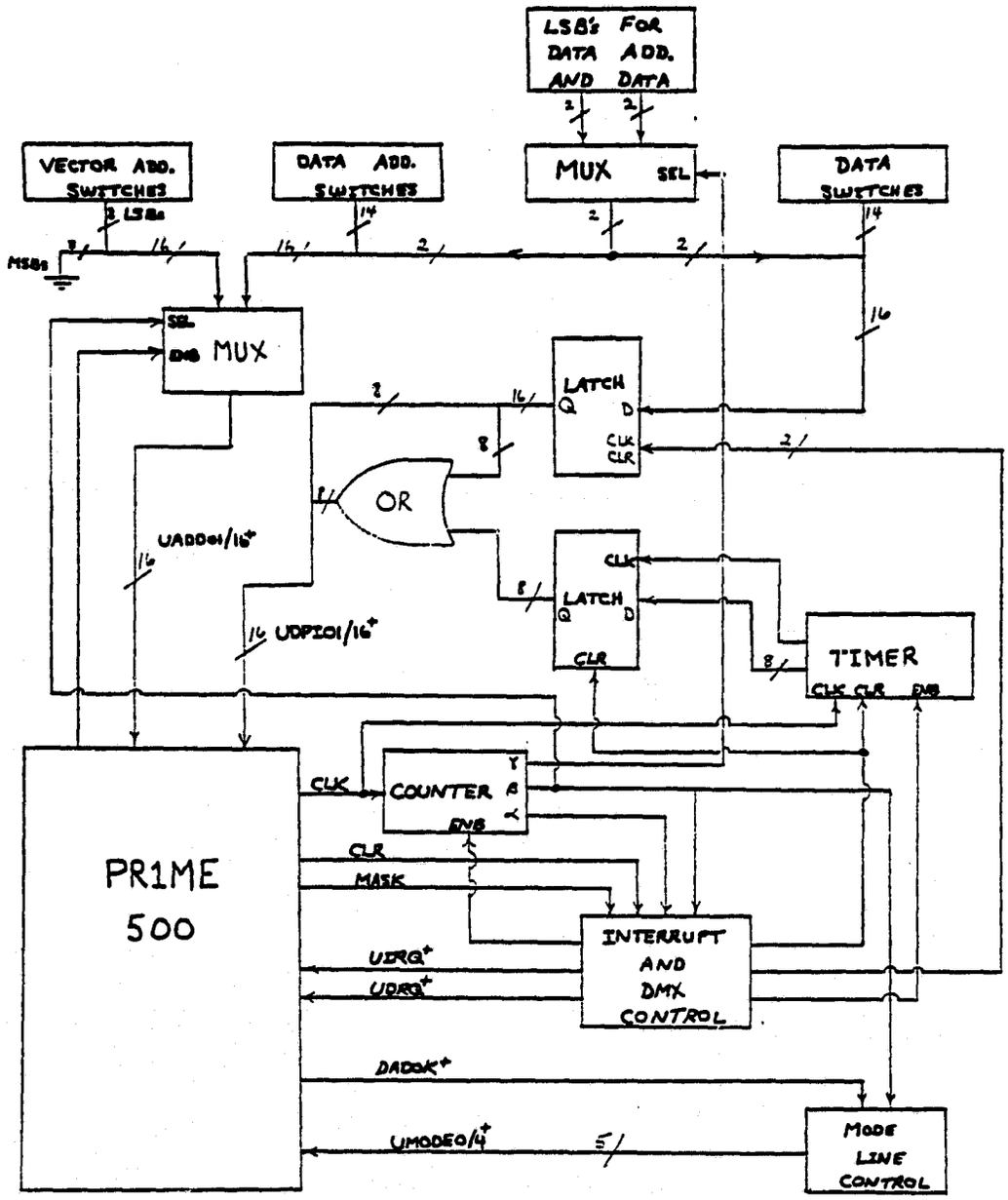

Figure 3.2. Data Emulator Block Diagram

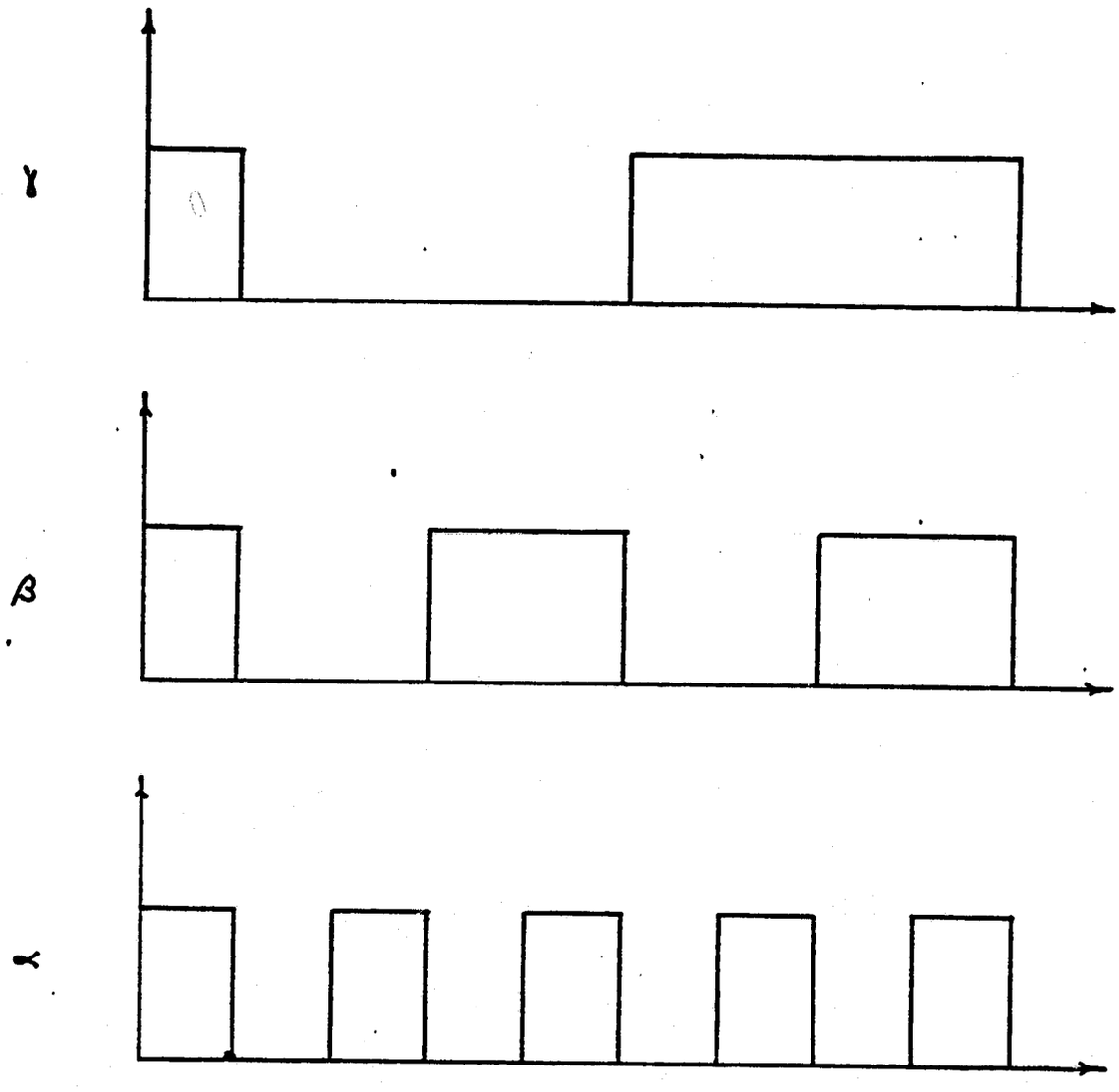

Figure 3.3. Unloaded Control Counter Outputs

the MSB.

The counter's alpha and beta outputs go to the Interrupt and DMX control circuitry. These lines determine when Interrupt and DMX requests occur, and insure that they do not happen at the same time. The beta output also goes to the Mode Line control electronics and to the multiplexer which selects which address will 'see' the bus. The beta output insures that when an Interrupt is taking place, the Interrupt address is on the address lines well before it is gated to the bus. Likewise it insures the Mode lines to be in the Interrupt Mode. When doing a DMX transfer, the beta line puts the DMX address on the address lines and sets the Mode well before they are gated to the bus. The counter does not advance unless the DMX transfer or Interrupt Request is finished. The gamma output picks which data word is being transferred.

The Interrupt and DMX control circuitry provides the actual Interrupt Requests ($UIRQ^{+}$) and DMX Requests ($UDRQ^{+}$). It enables the counter only after a process is complete. It also controls the Timer.

The Timer was installed to find out the approximate Interrupt processing time. When an Interrupt Request occurred the Timer or stopwatch was started. Just prior to leaving the Interrupt Service Routine the Timer was stopped and the time read. After this control was transferred back to the Data Emulator. The time read was usually on the order of 200 microseconds. This number has little significance now. The ISR used at the time this was measured will not be used in the final interface software. Figure 3.4 shows the Data Emulator's operating cycle and Figure 3.5 is a timing diagram for the Data Emulator. Detailed

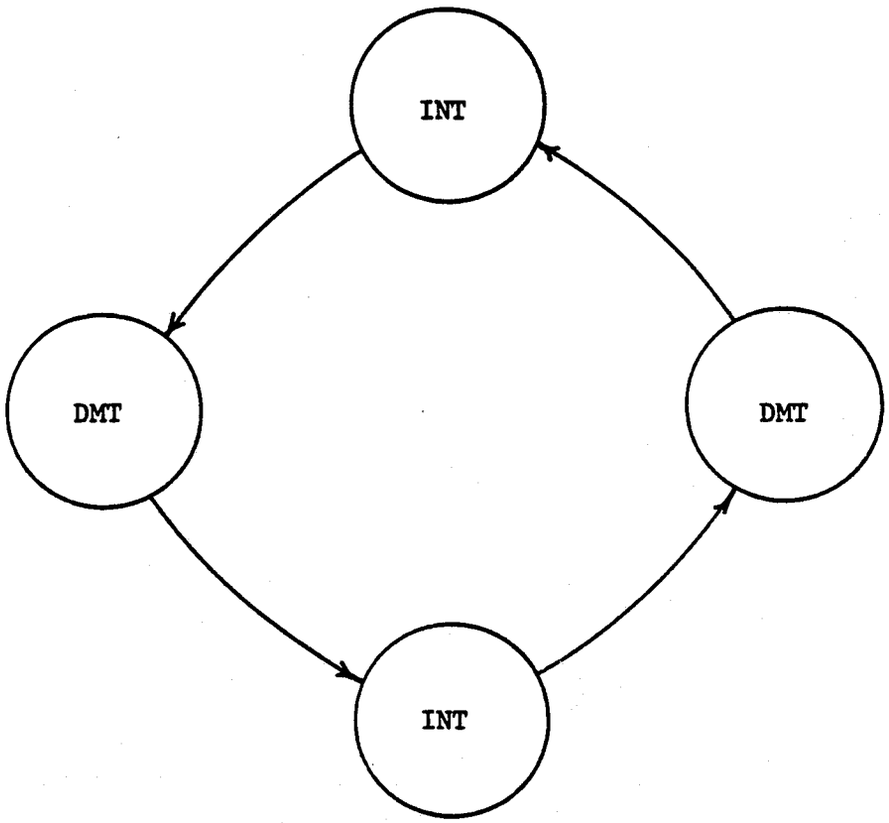

Figure 3.4. Data Emulator Operation Cycle

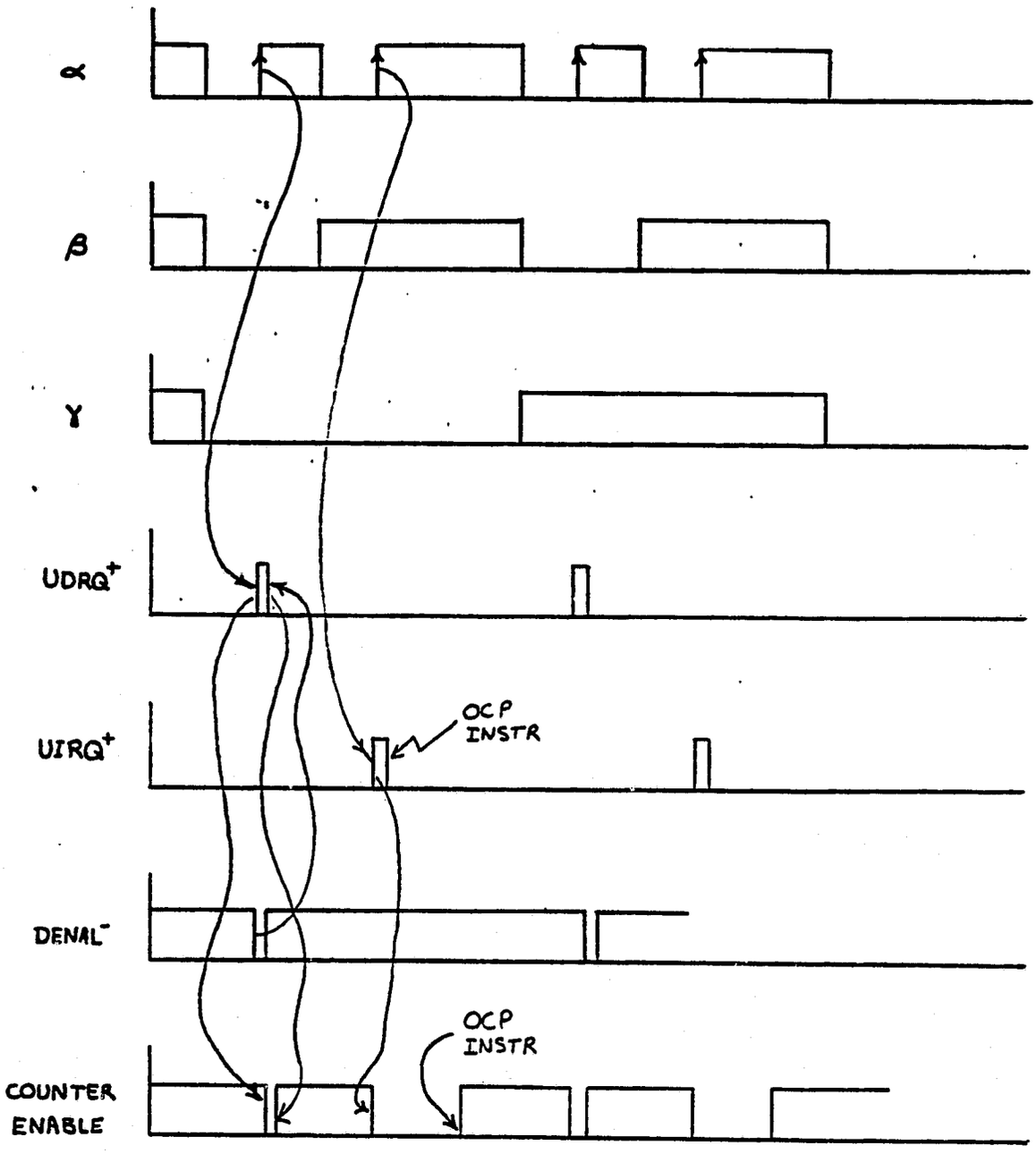

Figure 3.5. Timing Diagram for Data Emulator

circuit diagrams for this device are in the appendix.

3.3 The PRIME/Rover Interface

The primary functions of the PRIME/Rover Interface are as follow:

1.) To buffer data coming from the Rover via telemetry, such that little or no data will be lost. This is accomplished by using a bank of First In First Out memory chips (FIFOs).

2.) To transfer data into the right location in the computer's memory. Data is transferred into PRIME's memory by requesting a Direct Memory Transfer Cycle (DMT cycle). Its location in memory is partly specified by the computer and partly specified by address information coming from the Rover.

3.) It must signal the computer after transferring a complete block of data, such as an azimuth block, or when something goes wrong. In these situations the computer is signalled by an Interrupt Request. A status register tells the computer what caused the interrupt.

4.) It must be able to output commands back to the Rover. This is accomplished by using Programmed Input/Output (PIO) via a U/ART.

In addition to these primary functions the PRIME/Rover Interface has a number of other capabilities, the most important being that hardware can be 'data path diagnosed' by running a software package written by Michael Potmesil.

The amount of hardware had to be significantly increased to accomplish this, but debugging the Interface was vastly simplified as a

result. The additional hardware includes readback circuits on all the registers in the Interface. This allowed software to check such things as the DMT Address Register, the Command Register, the Vector Address and Mode Register, the Slot I.D. Register, and the Status Register. In addition to this, circuitry was added to load the FIFO memory banks from the computer. This allows software to check both the address and data FIFO buffers. In the future, this capability will enable one to check the software driver, T$ROVR, without having data coming from the Rover.

Construction of the PRIME/Rover Interface began in the middle of October 1979 and was completed in early November. On November 19 the Interface was found to be completely operational. It now has a permanent slot in the Image Processing Laboratory's PRIME 500 computer. Specifications of and complete circuit diagrams for this Interface are included in the Appendices.

3.4 Operating Principles

Figure 3.6 shows the relationship of the PRIME/Rover Interface to the whole system. Data comes from the Rover via telemetry in a serial format. Cipolle's electronics parallelizes the data and hands it to the PRIME/Rover Interface. The PRIME/Rover Interface then gives the data to the PRIME computer. Block diagrams for the Interface are given in Figure 3.7, Figure 3.8, and Figure 3.9. To understand how the Interface operates one must understand how the PRIME computer handles DMT cycles, Interrupt cycles and PIO. For a detailed description of these functions refer to the General Purpose Interface User's Guide listed in the reference.

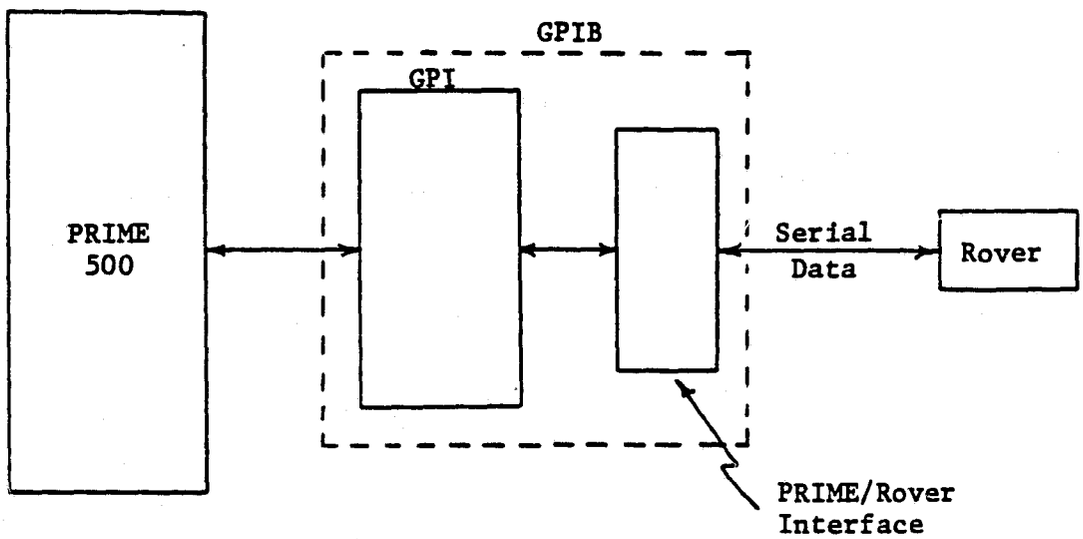

Figure 3.6. PRIME/Rover System Configuration

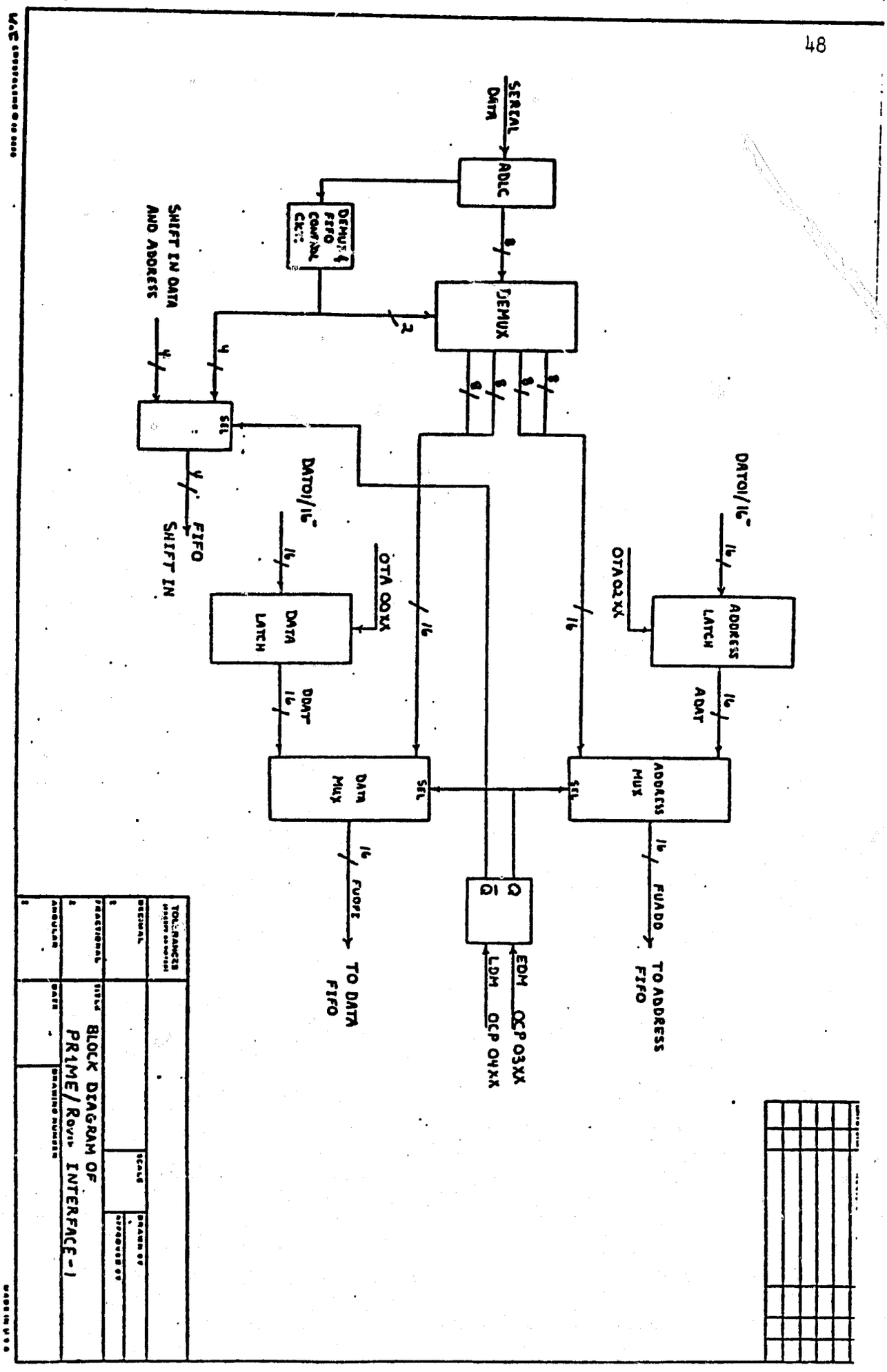

Figure 3.7. PRIME/Rover Interface Block Diagram - 1

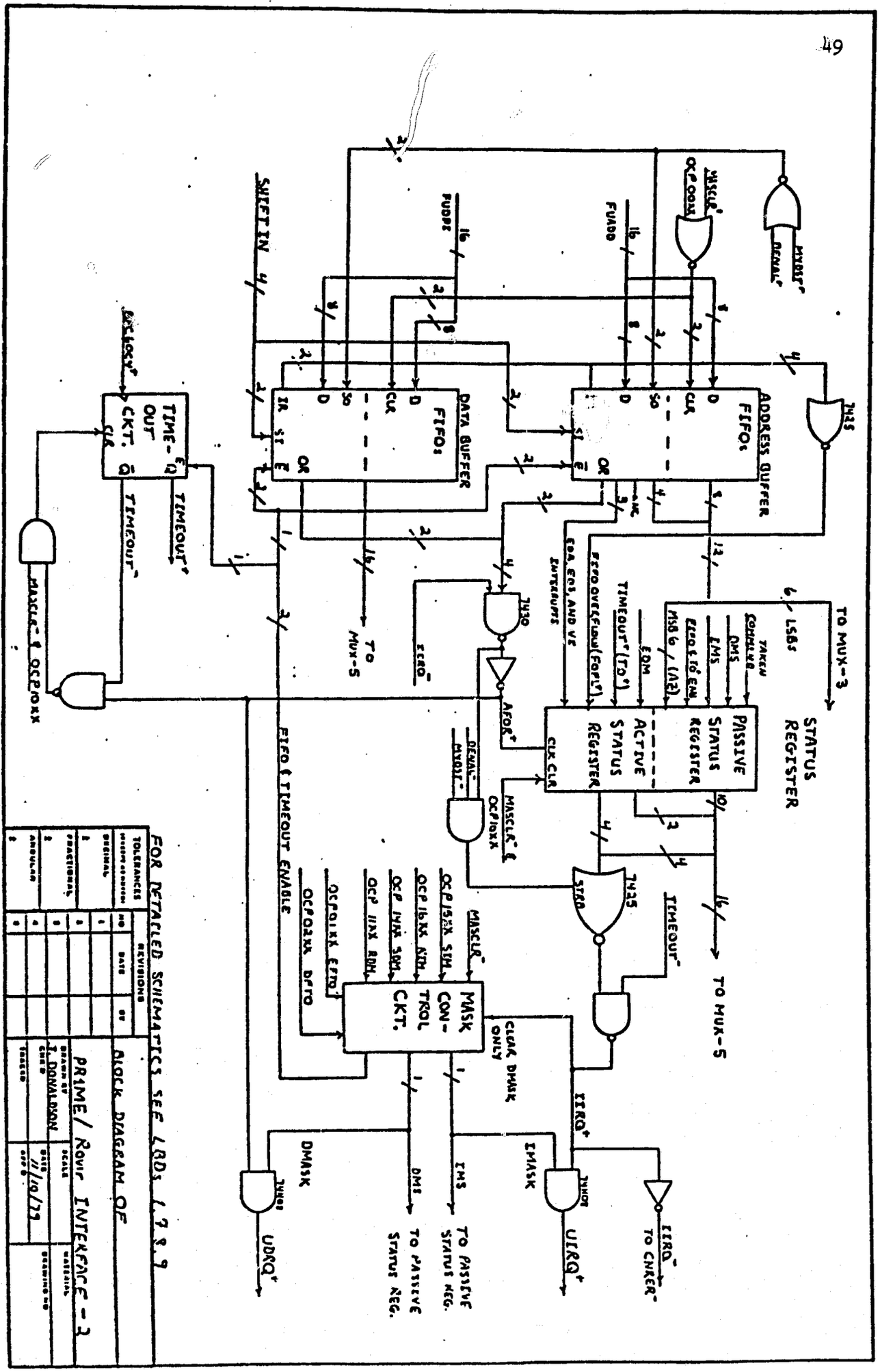

Figure 3.8. PRIME/Rover Interface Block Diagram - 2

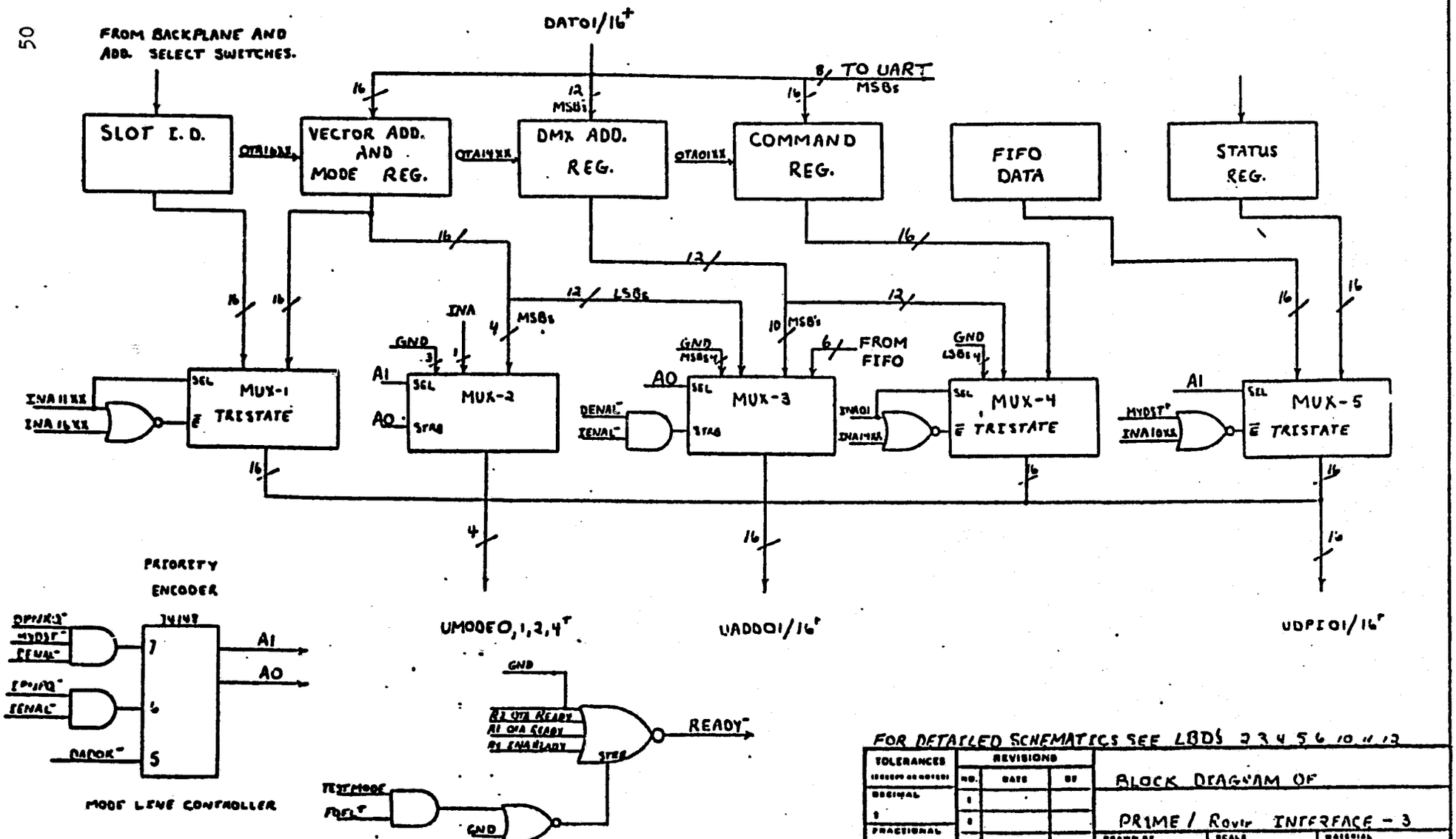

FOR DETAILED SCHEMATICS SEE LBDS 2 3 4 5 6 10 11 12

TOLERANCES	REVISIONS			BLOCK DIAGRAM OF
DECIMAL ±	NO.	DATE	BY	PRIME / Rover INTERFACE - 3
FRACTIONAL ±				DRAWN BY T. COWALDSON; SCALE; MATERIAL
ANGULAR ±				CHK'D; DATE 4/10/79; DRAWING NO
				ENGR'D; APP'D

Figure 3.9 PRIME/Rover Interface Block Diagram - 3

DMT Cycle

When a word has been loaded into the FIFOs it trickles through the FIFOs and the Output Ready (OR) outputs of the FIFOs go high. The FIFOs can be loaded by the ADLC or by the computer. When all the FIFO OR signals go high then $AFOR^-$ goes low. If the DMT mask is set, $UDRQ^+$ will go high, following $AFOR^+$. This signals the computer that the user is ready to transfer a word of data. When the computer is ready to take that word the $DENAL^-$ signal is asserted. This gates the address and mode information to the bus. The address tells the computer where we want to put the data, the mode tells it that we are interested in a DMT transaction. Soon after $DENAL^-$ is asserted, the signal $MYDST^+$ is asserted. This signal gates the data onto the bus. $DENAL^+$ and $MYDST^+$ are NORed to assert the Shift Out (SO) input of the FIFOs. If there is no Interrupt pending in the Active Status Register then the FIFOs will be free to transfer another word to memory as soon as it becomes available at the FIFO outputs. This sequence will continue until an Interrupt occurs.

Interrupt Cycle

All Interrupts except the Timeout Interrupt are clocked into a register by $AFOR^+$. These Interrupts are: 1) End of Scan (EOS); 2) End of Azimuth (EOA); 3) End of Vehicle Data (EOVD) and 4) FIFO overflow (FOFL). The outputs of this register are NORed. This NOR gate is inhibited by $AFOR^-$ and $DENAL^-$. This insures that Interrupts will occur only after a given DMT transfer is almost complete. The output of the NOR gate is NANDed with the $Timeout^-$ signal. The result is an effective OR of all five possible Interrupt conditions. The output of the NAND gate is called

IIRQ^{+}. If it goes high and if the Interrupt Mask is set, then UIRQ^{+} will be asserted. This signals the computer that an Interrupt is pending. It also resets the DMT mask, preventing any further DMT transactions. In addition to this it keeps AFOR^{+} unasserted. The siganl IENAL^{-} gates the Interrupt address to the bus. The first instruction in the Interrupt Service Routine resets the Interrupt mask by using an OCP instruction. Somewhere within the ISR the contents of the Status Register are read. The contents of the Status Register will indicate the Interrupt's cause. Prior to leaving the ISR the DMT mask is set. After this, DMT transactions will resume. A timing diagram showing the DMT and Interrupt timing sequence is given in Figure 3.10.

PIO Cycle

The general PIO cycle for the PRIME is illustrated in Figure 3.11. The Ready signal from the device, our Interface in this case, provides the handshake which allows the processor to know what to do next. If the Ready signal is asserted the strobe to the device is briefly asserted and the next instructing in software is skipped. If the Ready signal is unasserted, the next instruction in software is executed and no strobe pulse is issued.

3.5 Conclusion

Development of a reliable PRIME/Rover Interface was hindered for several months by flakey address line drivers in the PRIME constructed portion of the GPIB. This problem was resolved by replacing 4 I.C.'s. After eliminating this problem, work progressed rapidly on the PRIME/Rover Interface. This device has been constructed and all tests indicate it is

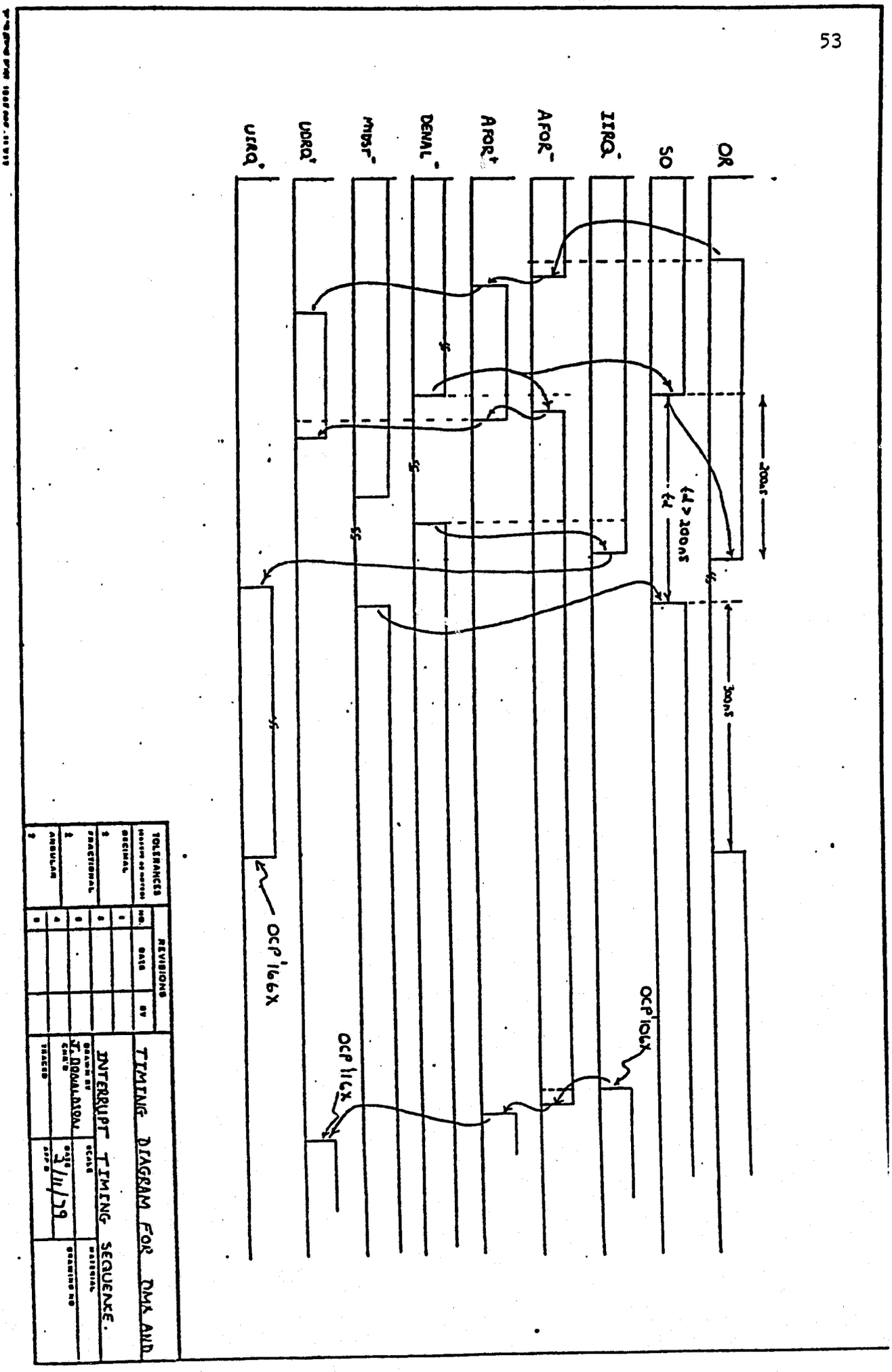

Figure 3.10. Timing Diagram for PRIME/Rover Interface

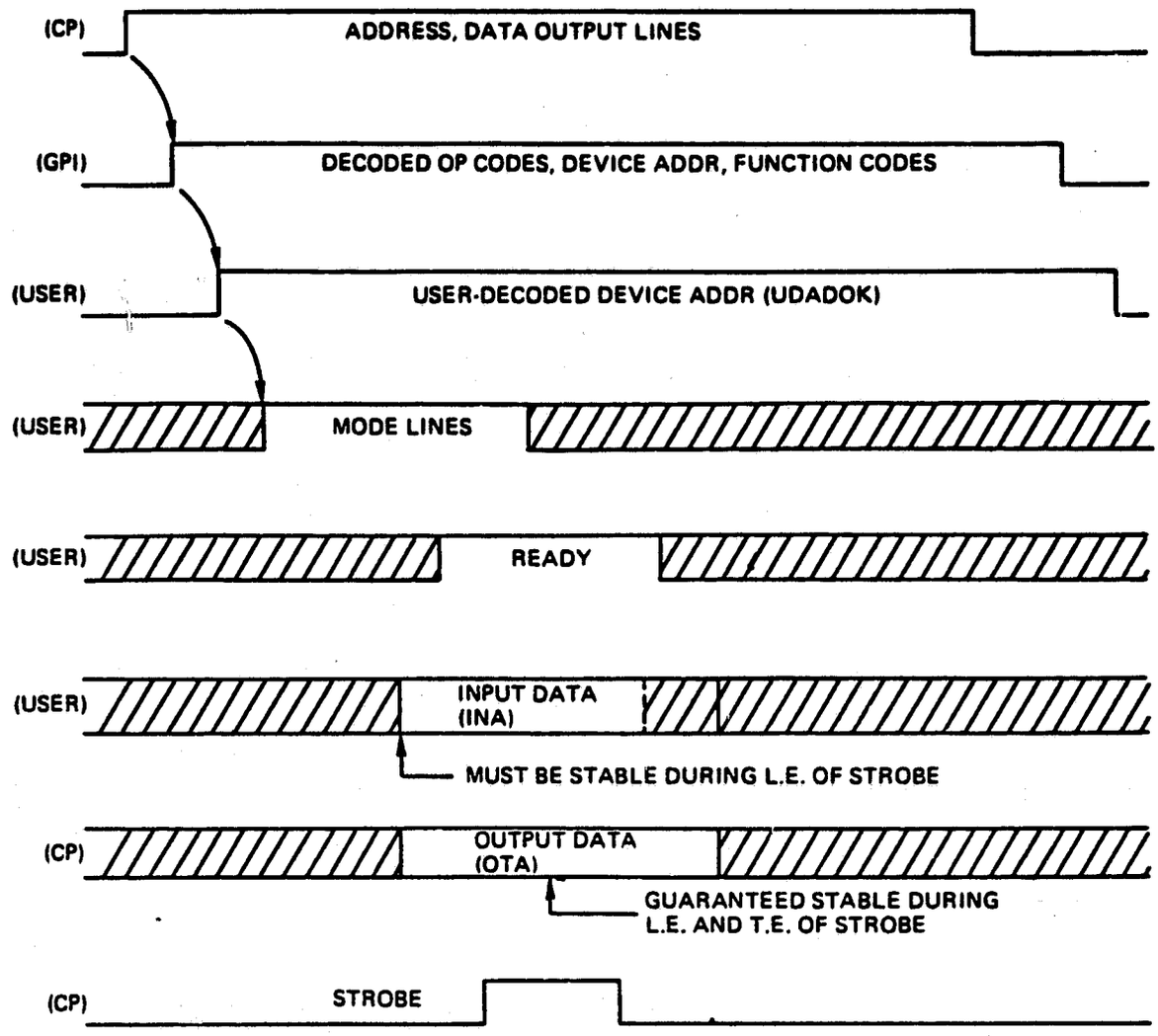

Figure 3.11. PIO Timing Sequence

operating as intended.

Before real data becomes available to the computer, at least two things must be done. First, T$ROVR, the I/O driver for the Interface, must be completed and debugged. This job is being done by Michael Potmesil. Second, the Telemetry link to the Interface must be finished and debugged. This work is being done by Dave Cipolle. Having completed these two tasks, one should be able to begin testing using the Platform designed by Gary Rich.

PART 4

LITERATURE CITED

1. Yerazunis, S., Autonomous Control of Roving Vehicles for Unmanned Exploration of the Planets - A Progress Report, R.P.I. Technical Report MP-603, Rensselaer Polytechnic Institute, Troy, N.Y., February 1979.

2. PRIME Computer, Inc., General Purpose Interface Users Guide, Revision 0, Prime Computer, Inc., 1976.

3. Texas Instruments, Inc., The TTL Data Book for Design Engineers, Second Edition, Texas Instruments, Inc., 1973.

4. Meshach, W., Elevation Scanning Laser/Detector Hazard Detection System: Pulsed Laser and Photodetector Components, Rensselaer Polytechnic Institute, Troy, N.Y., June 1978.

5. Coles, G., Real-Time Operating System for a Multi-Laser/Multi-Detector System, Rensselaer Polytechnic Institute, Troy, N.Y., December 1979.

6. PRIME Computer, Inc., Reference Guide, System Architecture and Instructions IDR 3060, First Printing, Prime Computer, Inc., July 1978.

7. Craig, J., Elevation Scanning Laser/Multi-Sensor Hazard Detection System, Rensselaer Polytechnic Institute, Troy, N.Y., August 1978.

8. Turner, J., A Propulsion and Steering Control System, Rensselaer Polytechnic Institute, Troy, N.Y., August 1979.

9. Cipole, D., Telemetry Data Link System, Rensselaer Polytechnic nstitute, Troy, N.Y., May 1979.

Appendix 5.1
PRIME/Rover Interface Specifications

REGISTER DEFINITIONS

There are five registers in the user designed portion of the Interface. They are listed below.

1.)	Slot I.D. and Device I.D. Register	'116X
2.)	Command Register	'016X
3.)	DMT/Address Register	'146X
4.)	Status Register	'106X
5.)	Vector Address and Mode Register	'166X

1.) Slot I.D. and Device I.D. Register (Read Only)

This information comes directly from the backplane and from the switches that determine the Device Code. This information is available to the user by issuing a INA '116X. For a detailed description of how this Register is set up, see the following figure.

SLOT I.D. AND DEVICE I.D. REGISTER

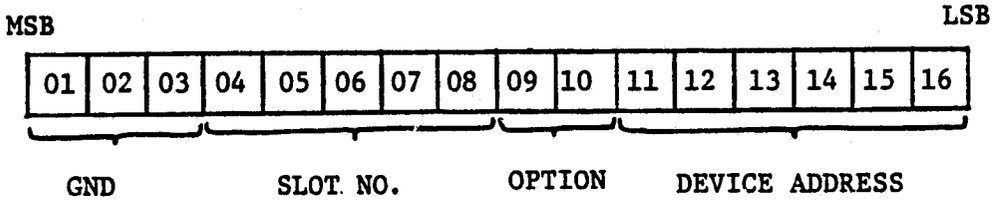

Device Address for PRIME/Rover Interface = 63.

2.) Command Register (Read and Write)

This Register is loaded by issuing a OTA '016X. The top or upper eight bits of anything loaded into this Register will be transmitted to the Mars Rover. It is also possible to read back any command sent. One accomplishes this by issuing a INA '016X. This enters all 16 bits of the Command Register, not just the upper eight bits which are actually transmitted to the Rover. The following figure illustrates how the Command Register is set up.

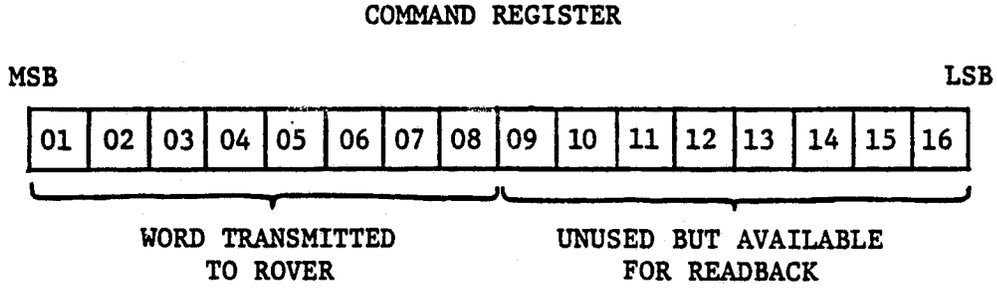

3.) DMT Address Register (Limited Read and Write)

One loads this Register by issuing a OTA '146X. At present the Register is only 12 bits wide and is equipped to load only the upper 12 bits of the 'A' Register. This is configured as it is to provide those users doing DMTs some versatility in their choice of how many bits of address they will supply. In the future if one desires to do DMAs or DMCs, it can easily be arranged by widening this Register to the full 16 bits.

In our application the top ten bits of this Register will be used as DMT address bits. The bottom six bits will come from the Mars Rover.

To read back the contents of this Register one must issue a INA '146X. The following figure illustrates how the DMT Register is set up.

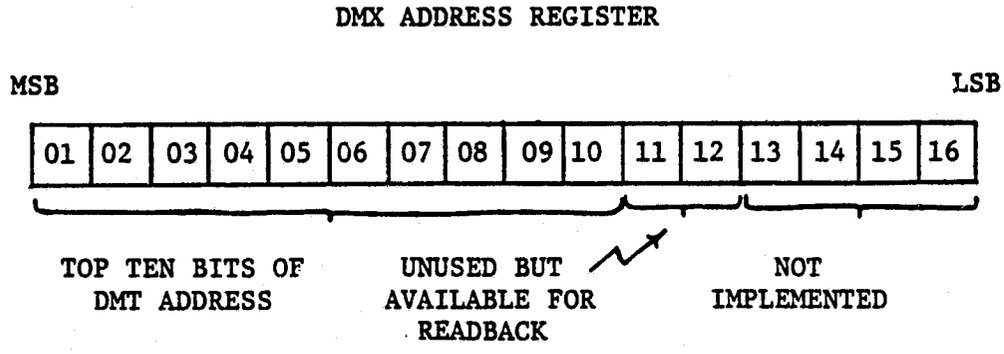

4.) Status Register (Read Only)

The Status Register's general configuration is illustrated in the following figure. Its contents are available for read back using a INA '106X.

The Active Status Register is defined as that portion of the Status Register whose bits, when they go high, will produce an Interrupt Request. The Passive Status Register bits will not cause an Interrupt Request on going high but instead will give some indication of the Interface's Status. A complete list of the Status Register bits, showing what they do or indicate about the state of the Interface, is given on page 63.

STATUS REGISTER

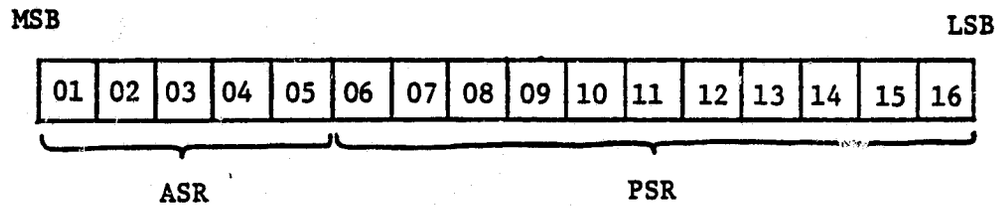

ASR = ACTIVE STATUS REGISTER

PSR = PASSIVE STATUS REGISTER

STATUS REGISTER

ACTIVE STATUS REGISTER

MSB	Bit 01 - END OF VEHICLE DATA	(EOVD)
	Bit 02 - END OF SCAN	(EOS)
	Bit 03 - END OF AZIMUTH	(EOA)
	Bit 04 - FIFO OVERFLOW	(FOFL)
	Bit 05 - TIMEOUT	(TO)

PASSIVE STATUS REGISTER

	Bit 06 - DIAGNOSTIC MODE ENABLED	
	Bit 07 - BACK OF SCAN	
	Bit 08 - AZIMUTH BIT 01	(MSB)
	Bit 09 - AZIMUTH BIT 02	
	Bit 10 - AZIMUTH BIT 03	
	Bit 11 - AZIMUTH BIT 04	
	Bit 12 - AZIMUTH BIT 05	(LSB)
	Bit 13 - COMMAND TAKEN	
	Bit 14 - INTERRUPT MASK SET	
	Bit 15 - DMx MASK SET	
LSB	Bit 16 - TIMEOUT CIRCUIT ENABLED	

5.) Vector Address and Mode Register (Read and Write)

This Register is loaded by issuing a OTA '166X. Read back is accomplished by issuing a INA '166X. The format for this Register is illustrated in the following figure.

VECTOR ADDRESS AND MODE REGISTER

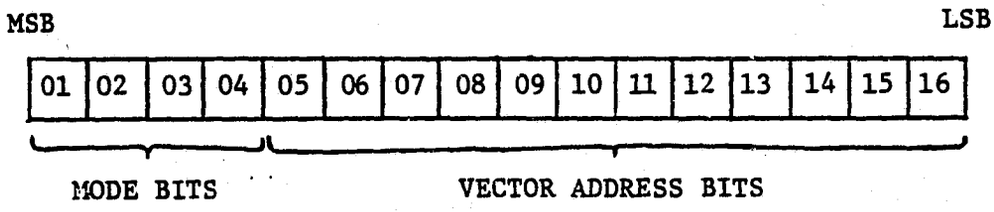

PROGRAMMING

Below is a list of the instruction set implemented by this Interface.

OTA '006X Load FIFO Data Buffer

OTA '016X Output to Command Register and U/ART

OTA '026X Load FIFO Address Buffer

OTA '146X Load DMT Address

OTA '166X Load Interrupt Vector Address and Mode

INA '016X Input Command Sent

INA '106X Input Status

INA '116X Input Slot I.D. and Device I.D.

INA '146X Input DMT Address

INA '166X Input Interrupt Vector Address

OCP '006X Clear FIFOs

OCP '016X Enable Timeout

OCP '026X Disable Timeout

OCP '036X Enter Diagnostic Mode

OCP '046X Leave Diagnostic Mode

OCP '106X Clear Status Register

OCP '116X Enable DMx

OCP '146X Disable DMx

OCP '156X Set Interrupt Mask

OCP '166X Clear Interrupt Mask

OCP '176X Initialize

Appendix 5.2
Circuit Diagrams for PRIME/Rover Interface

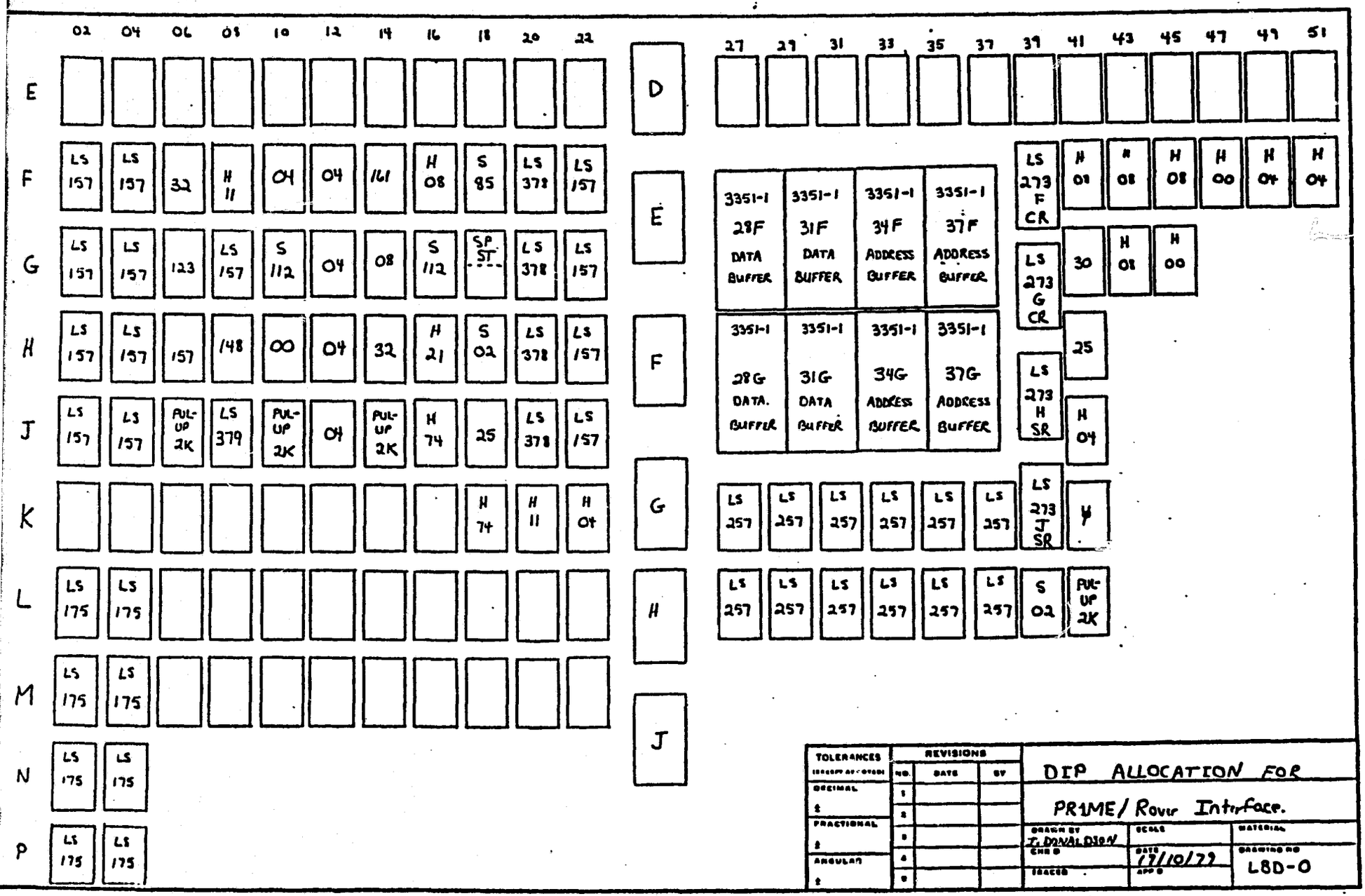
02 04 06 08 10 12 14 16 18 20 22
E
F LS 157 | LS 157 | 32 | H 11 | 04 | 04 | 161 | H 08 | S 85 | LS 378 | LS 157
G LS 157 | LS 157 | 123 | LS 157 | S 112 | 04 | 08 | S 112 | SP ST | LS 378 | LS 157
H LS 157 | LS 157 | 157 | 148 | 00 | 04 | 32 | H 21 | S 02 | LS 378 | LS 157
J LS 157 | LS 157 | PUL-UP 2K | LS 379 | PUL-UP 2K | 04 | PUL-UP 2K | H 74 | 25 | LS 378 | LS 157
K | | | | | | | | H 74 | H 11 | H 04
L LS 175 | LS 175
M LS 175 | LS 175
N LS 175 | LS 175
P LS 175 | LS 175
D
E
F
G
H
J
27 29 31 33 35 37 39 41 43 45 47 49 51
3351-1 28F DATA BUFFER | 3351-1 31F DATA BUFFER | 3351-1 34F ADDRESS BUFFER | 3351-1 37F ADDRESS BUFFER
3351-1 28G DATA. BUFFER | 3351-1 31G DATA BUFFER | 3351-1 34G ADDRESS BUFFER | 3351-1 37G ADDRESS BUFFER
LS 257 | LS 257 | LS 257 | LS 257 | LS 257 | LS 257
LS 257 | LS 257 | LS 257 | LS 257 | LS 257 | LS 257
LS 273 F CR | H 08 | H 08 | H 08 | H 00 | H 04 | H 04
LS 273 G CR | 30 | H 08 | H 00
LS 273 H SR | 25 | H 04
LS 273 J SR | H
S 02 | PUL-UP 2K
TOLERANCES
DECIMAL
FRACTIONAL
ANGULAR
REVISIONS
NO. DATE BY
DIP ALLOCATION FOR
PRIME/Rover Interface.
DRAWN BY T. DONALDSON
CHK'D
TRACED
SCALE
DATE 17/10/79
APP'D
MATERIAL
DRAWING NO L8D-0

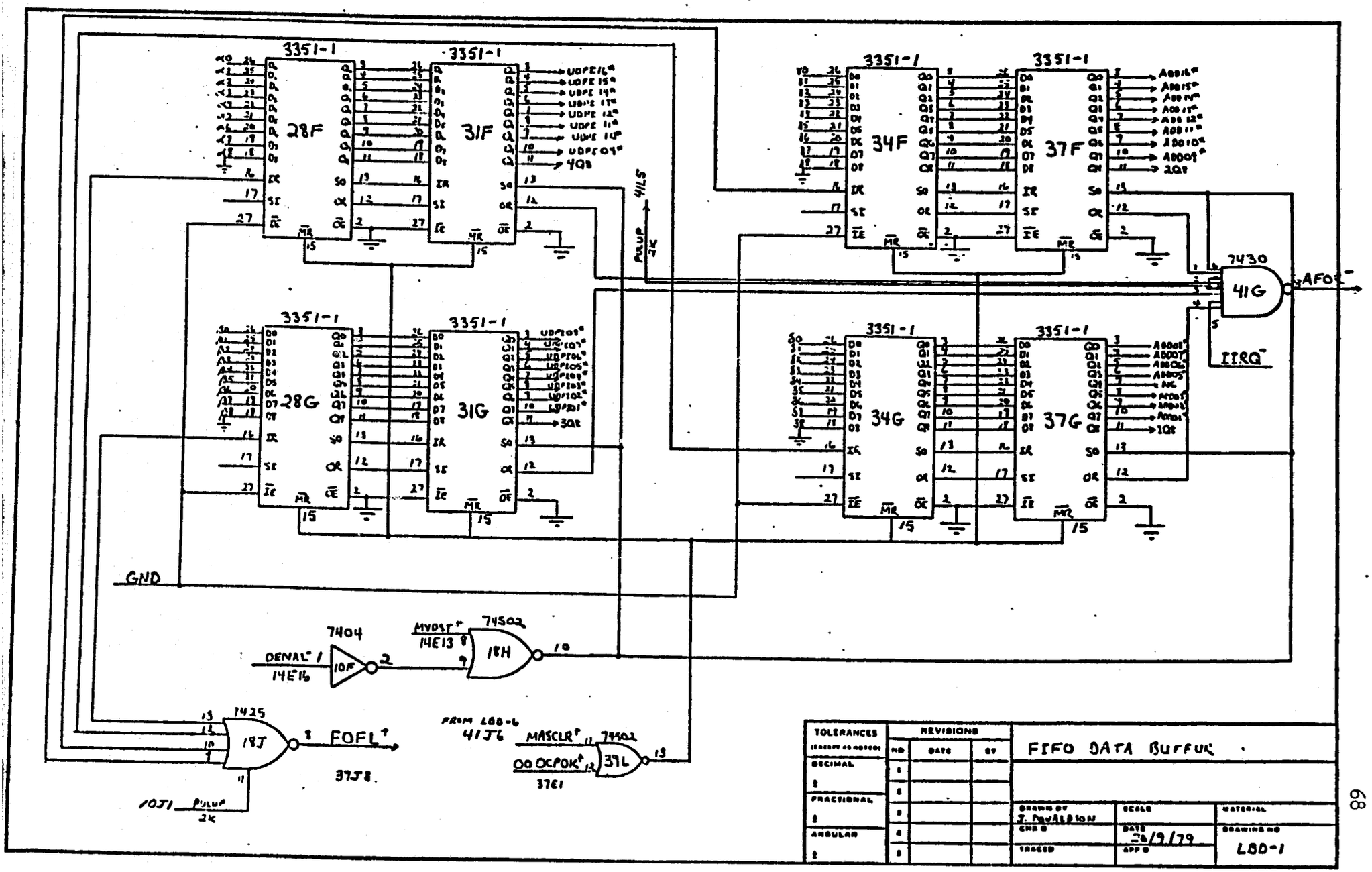
3351-1
28F
31F
34F
37F
28G
31G
34G
37G
7430
41G
AFOL
IIRQ
7404
10F
74S02
18H
7425
18J
FOFL
37J8
GND
PULLUP 2K
FROM L00-6
41J6
MASCLR
OD OCPOK
37E1
37L
TOLERANCES
REVISIONS
NO
DATE
BY
DECIMAL
FRACTIONAL
ANGULAR
FIFO DATA BUFFER
DRAWN BY
J. RAVALESON
SCALE
MATERIAL
CHK'D
DATE
7/9/79
DRAWING NO
L00-1
TRACED
APP'D

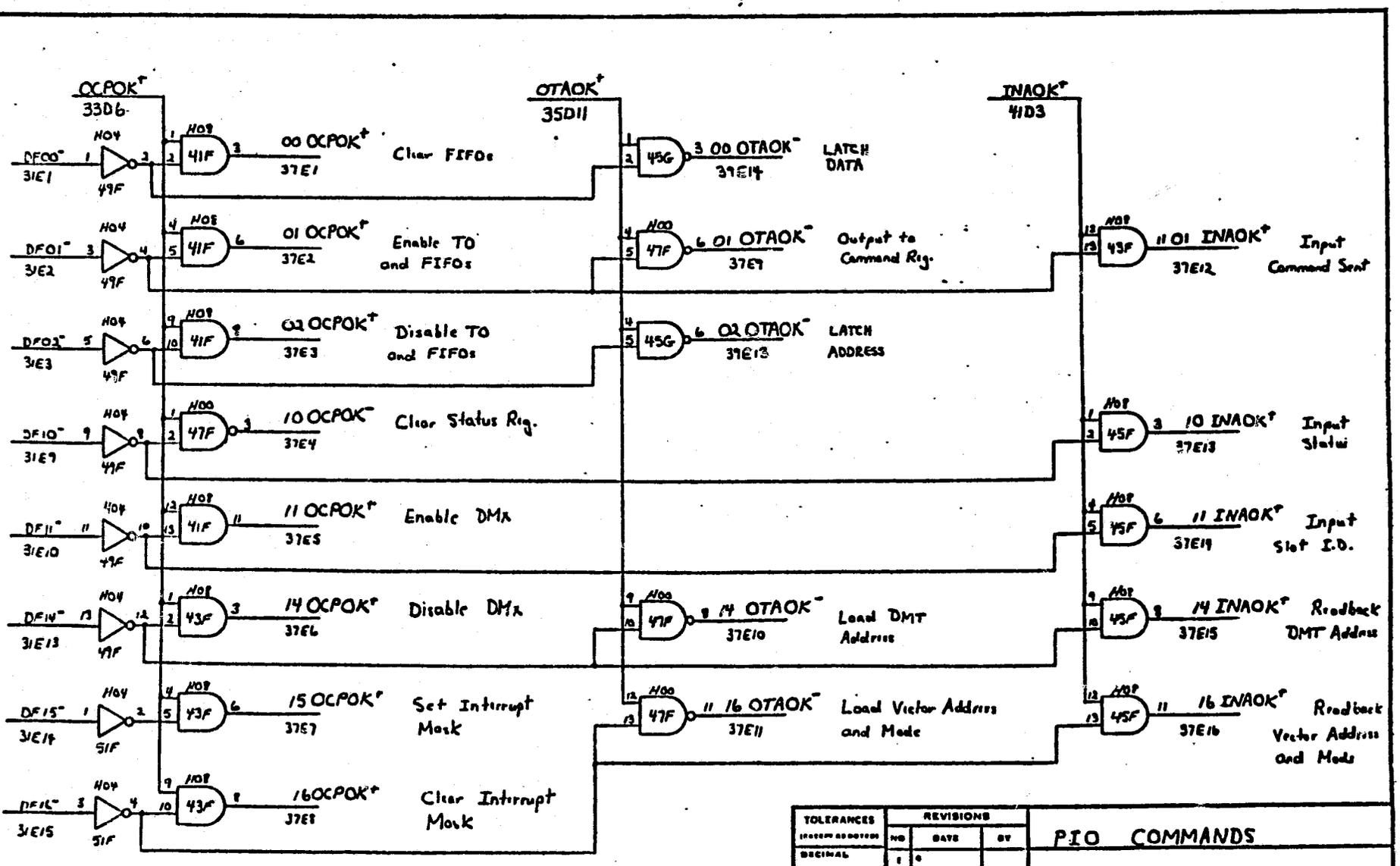

TOLERANCES	REVISIONS			PIO COMMANDS		
DECIMAL	NO	DATE	BY			
FRACTIONAL						
ANGULAR				DRAWN BY T. DONALDSON	SCALE	MATERIAL
				CHK'D	DATE 13/10/79	DRAWING NO 180-2
				TRACED	APP'D	

DATE	APP	REVISION RECORD	AUTH	DR	CK

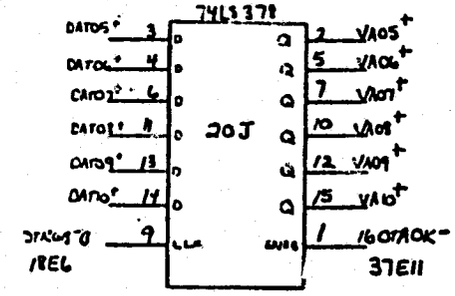

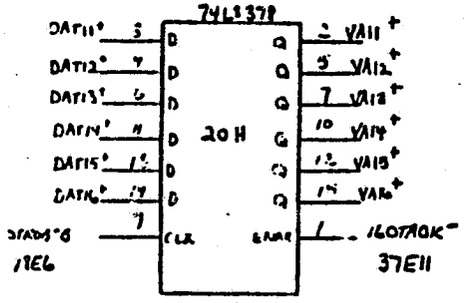

LOAD VECTOR ADDRESS

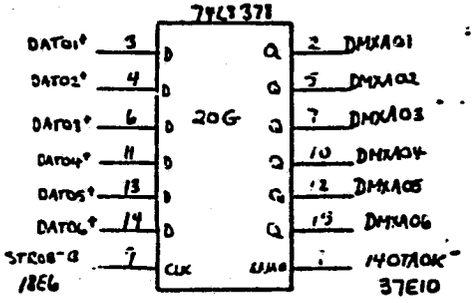

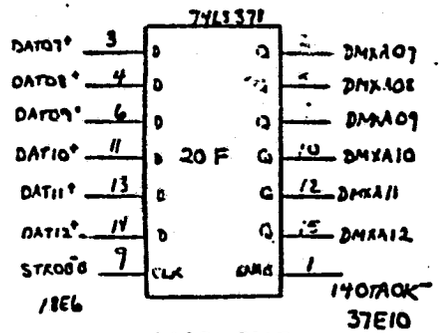

LOAD DMT ADDRESS

TOLERANCES UNLESS OTHERWISE NOTED			
DECIMAL ±		SCALE	DRAWN BY J. SWALDSON
			APPROVED BY
FRACTIONAL ±	TITLE VECTOR AND DMA ADDRESS REGISTERS		
ANGULAR ±	DATE 30/4/79	DRAWING NUMBER L80-3	

	4	5	6	7	A1	A0	UMODEX	UADD
DMT	X	X	X	L	L	L	'A'	'A'
INT	X	X	L	H	L	H	L	'B'
PIO	X	L	H	H	H	L	'B'	'A'
REST	L	H	H	H	H	H	L	'B'

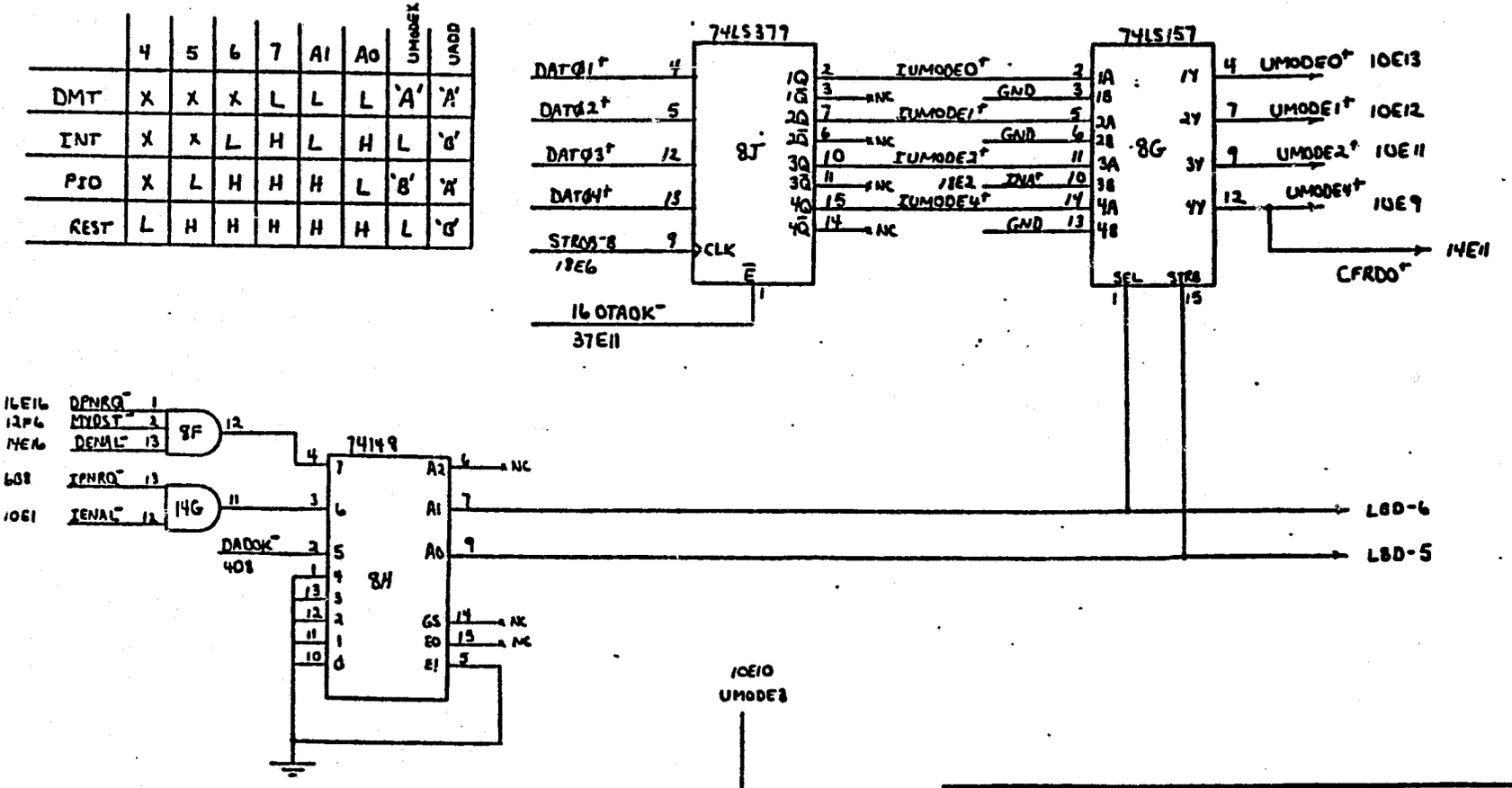

TOLERANCES	REVISIONS			MODE LINE CONTROL CKTRY		
DECIMAL ±	NO	DATE	BY			
FRACTIONAL ±				DRAWN BY T. DONALDSON	SCALE	MATERIAL
ANGULAR ±				CHK'D	DATE 4/3/79	DRAWING NO L8D-4
				TRACED	APP'D	

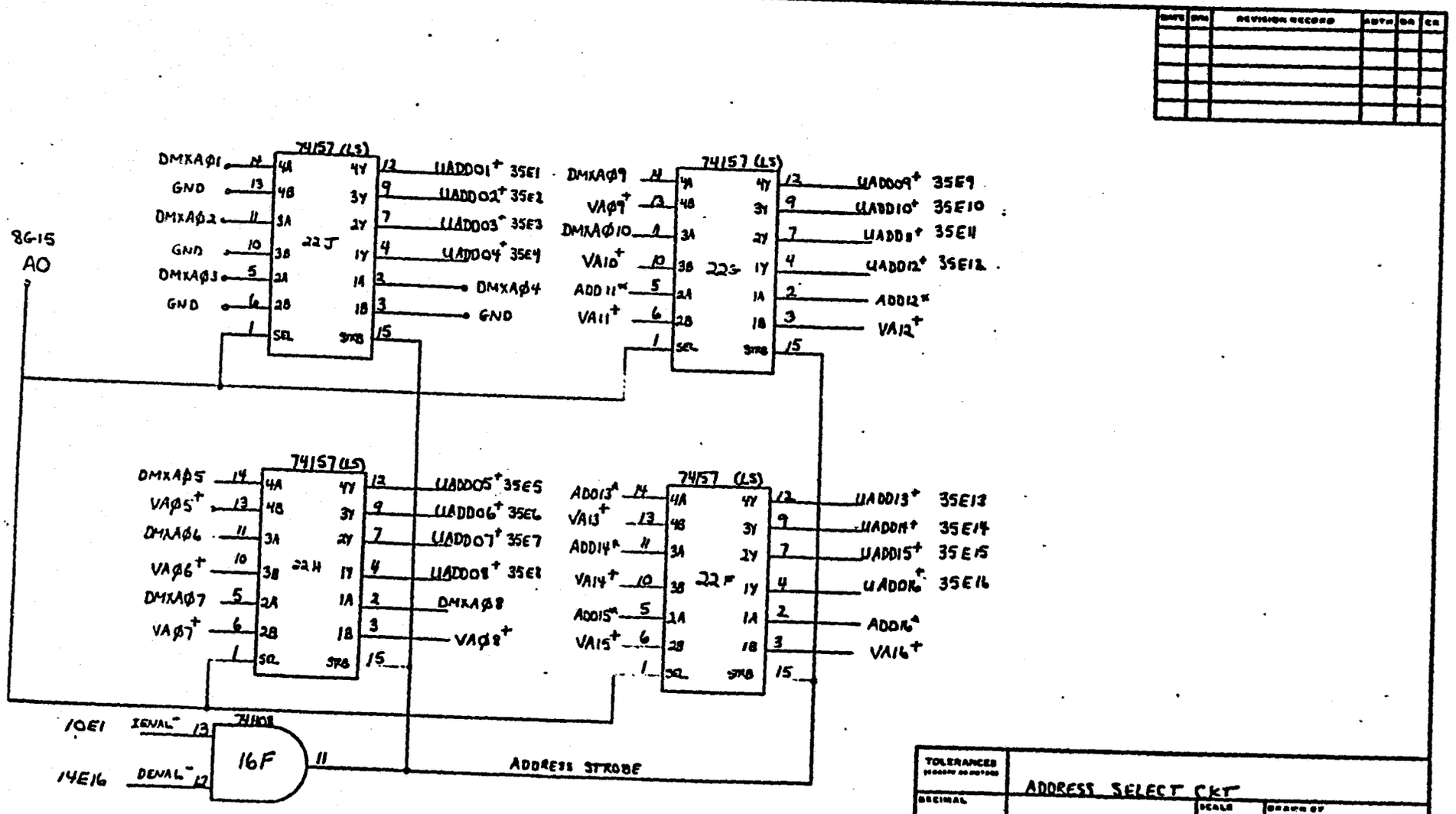

DATE	BY	REVISION RECORD	APP'D	CK	ECR

TOLERANCES	ADDRESS SELECT CKT		
DECIMAL		SCALE	DRAWN BY T SWANSON
FRACTIONAL	TITLE		APPROVED BY
ANGULAR	DATE 21/4/79	DRAWING NUMBER LBD-5	

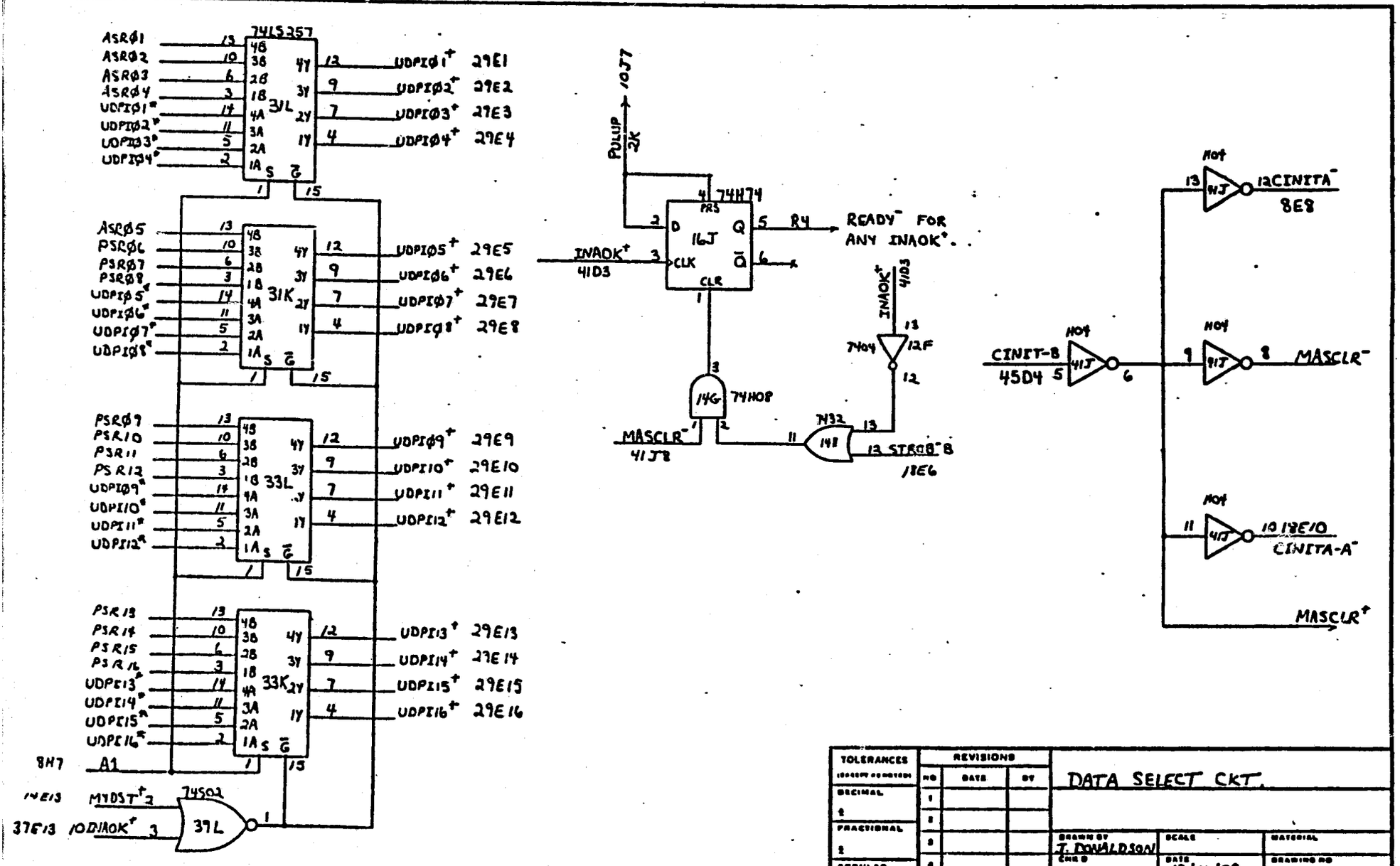

TOLERANCES	REVISIONS			DATA SELECT CKT.			
DECIMAL ±	NO	DATE	BY				
FRACTIONAL ±	1						
ANGULAR ±	2						
	3			DRAWN BY T. DONALDSON	SCALE	MATERIAL	
	4			CHK'D	DATE 12/10/79	DRAWING NO L80-6	
	5			TRACED	APP'D		

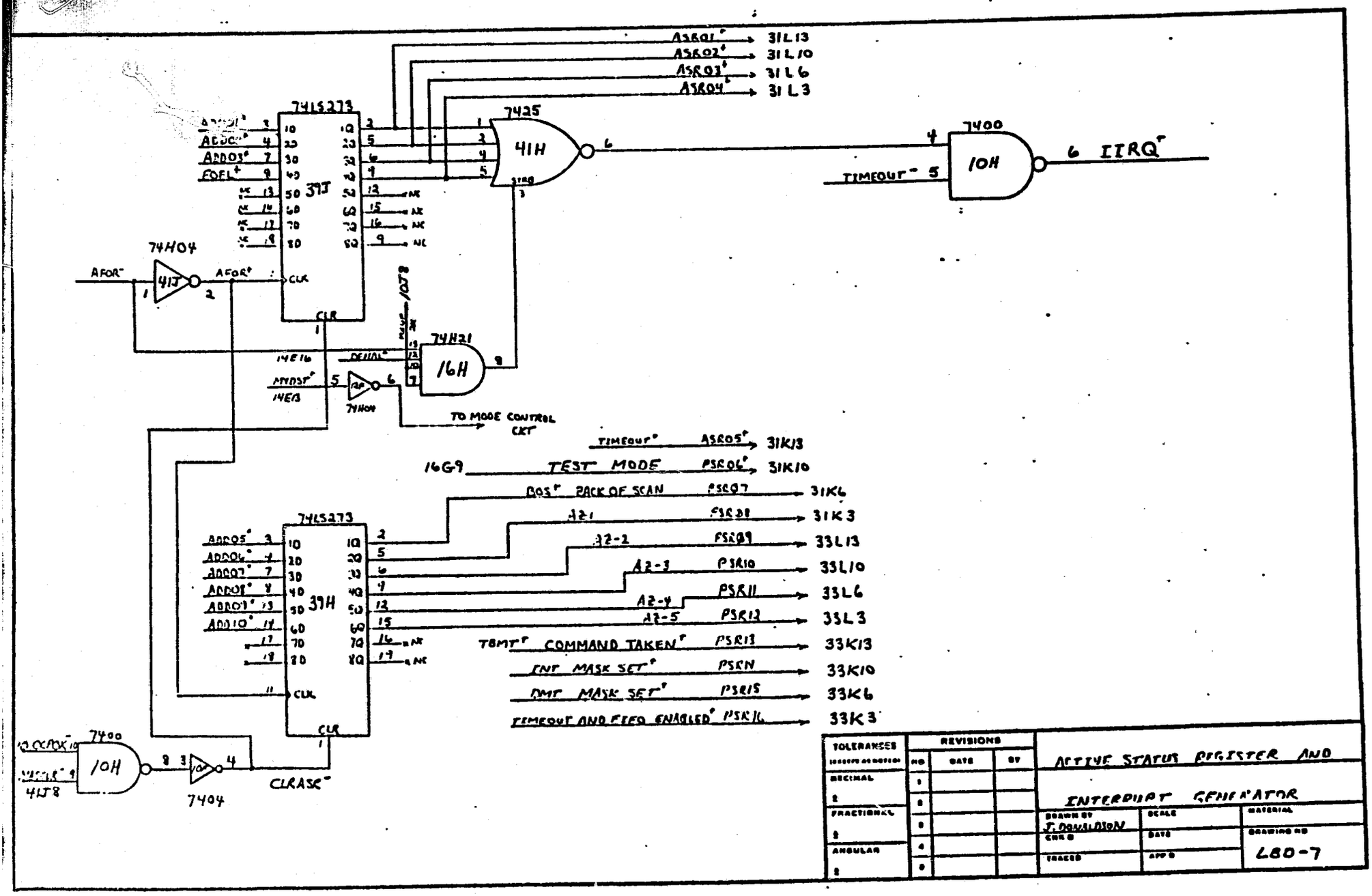

TOLERANCES	REVISIONS			ACTIVE STATUS REGISTER AND INTERRUPT GENERATOR		
DECIMAL	NO	DATE	BY			
FRACTIONAL				DRAWN BY F. DAWLIDSON	SCALE	MATERIAL
ANGULAR				CHK'D	DATE	DRAWING NO LBD-7
				TRACED	APP'D	

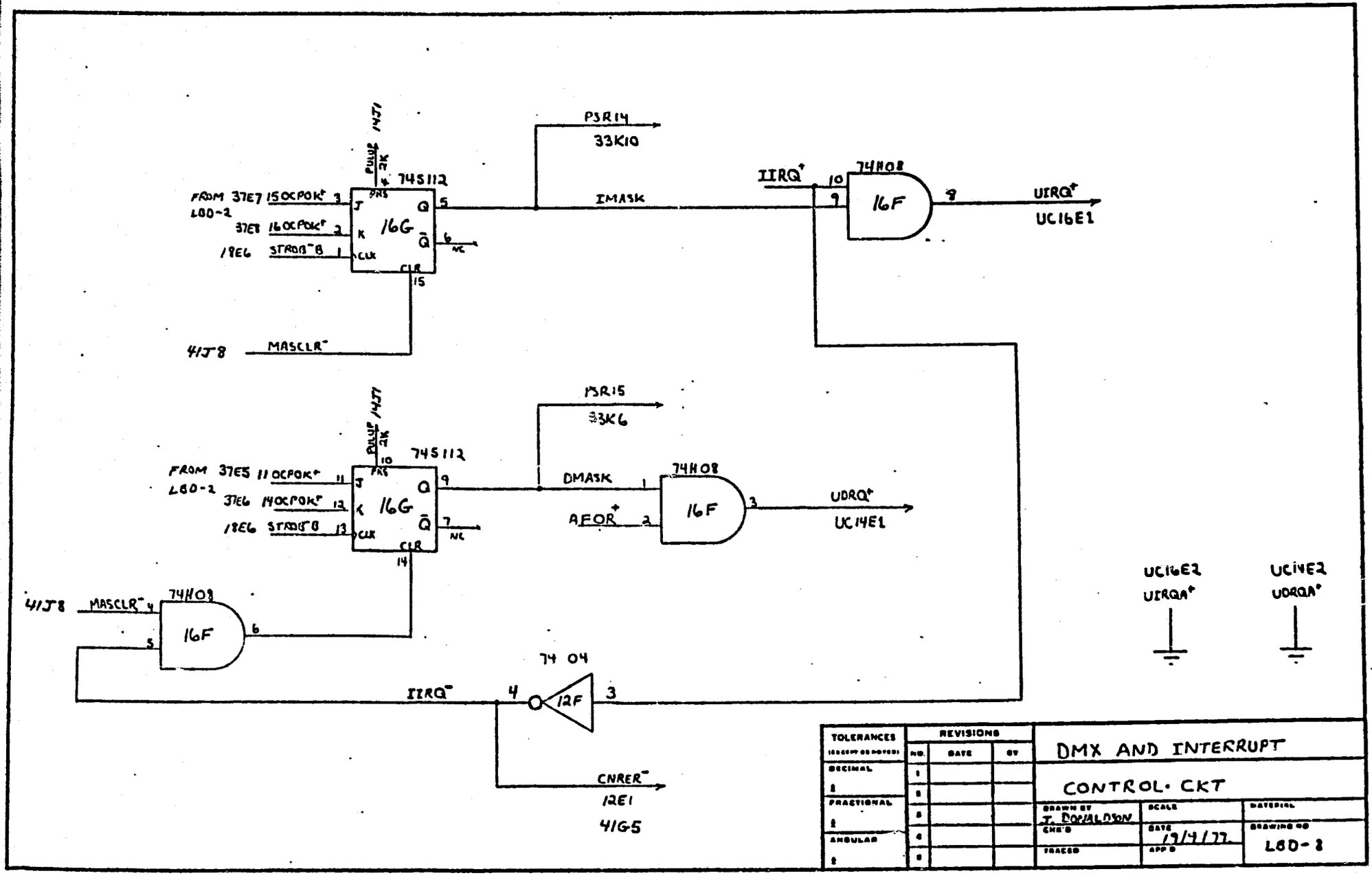

TOLERANCES	REVISIONS			DMX AND INTERRUPT
DECIMAL	NO.	DATE	BY	CONTROL CKT
FRACTIONAL				DRAWN BY: T. DONALDSON; SCALE; MATERIAL
ANGULAR				CHK'D; DATE: 12/4/77; DRAWING NO: L60-8
				TRACED; APP'D

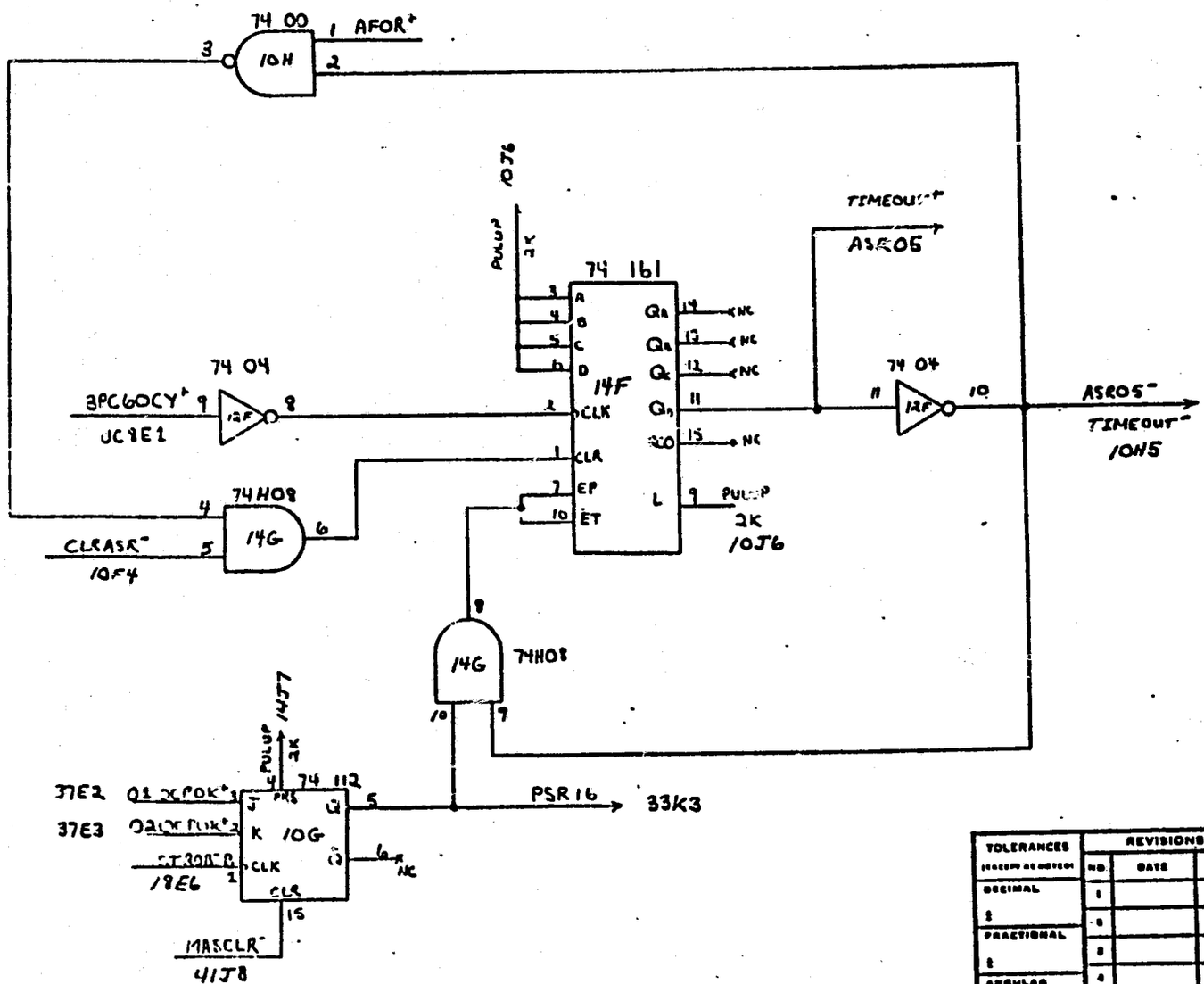

TOLERANCES	REVISIONS			TIMEOUT CKT		
DECIMAL	NO.	DATE	BY			
FRACTIONAL	1					
ANGULAR	2					
	3					
	4					
	5					
				DRAWN BY J. DONALDSON	SCALE	MATERIAL
				CHK'D	DATE 4/7/79	DRAWING NO L8D-9
				TRACED	APP'D	

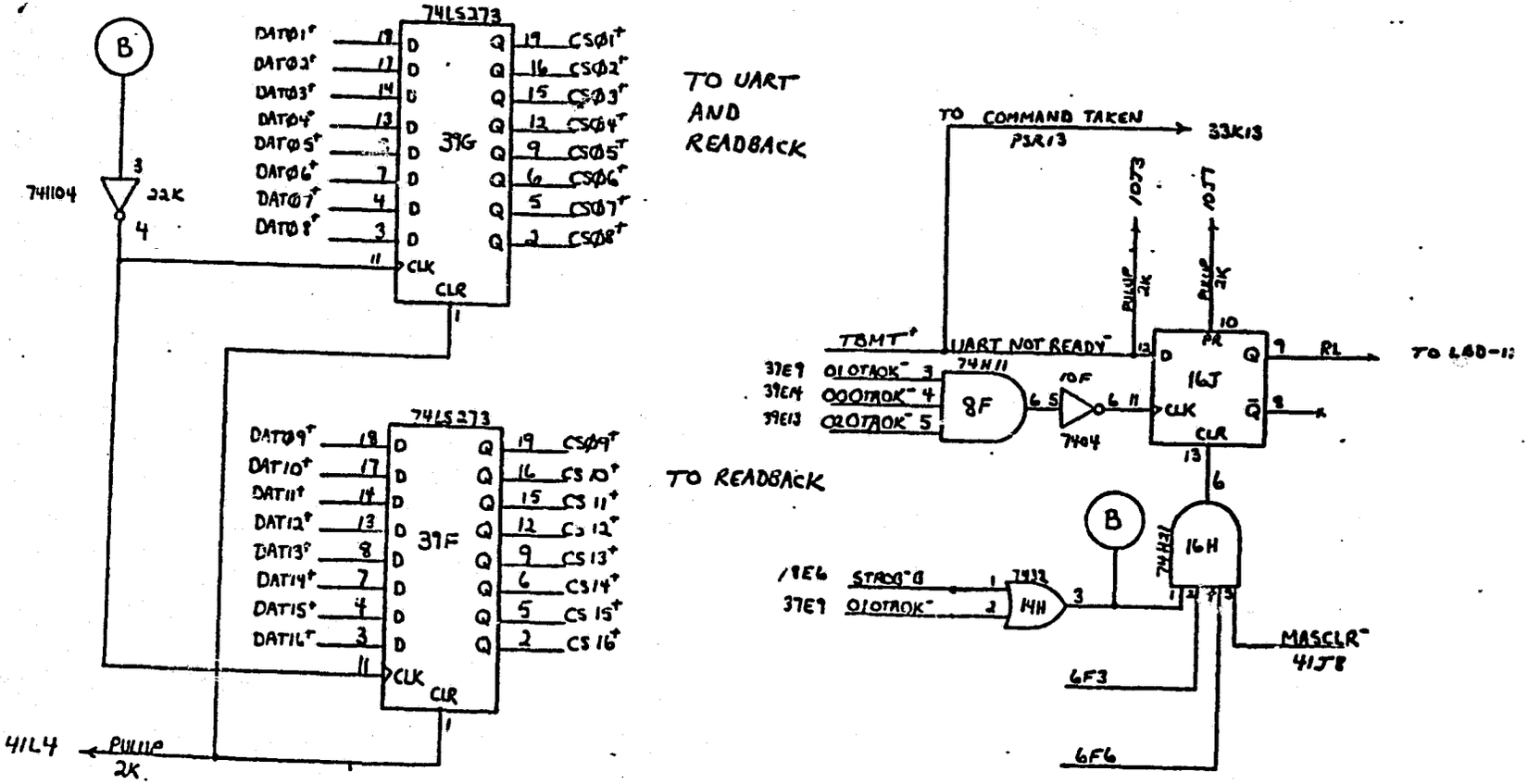

TOLERANCES	REVISIONS			COMMAND REGISTERS		
DECIMAL ±	NO	DATE	BY			
FRACTIONAL ±						
ANGULAR ±				DRAWN BY T. DONALDSON	SCALE	MATERIAL
				CHK'D	DATE 14/10/79	DRAWING NO LAD-10
				TRACED	APP'D	

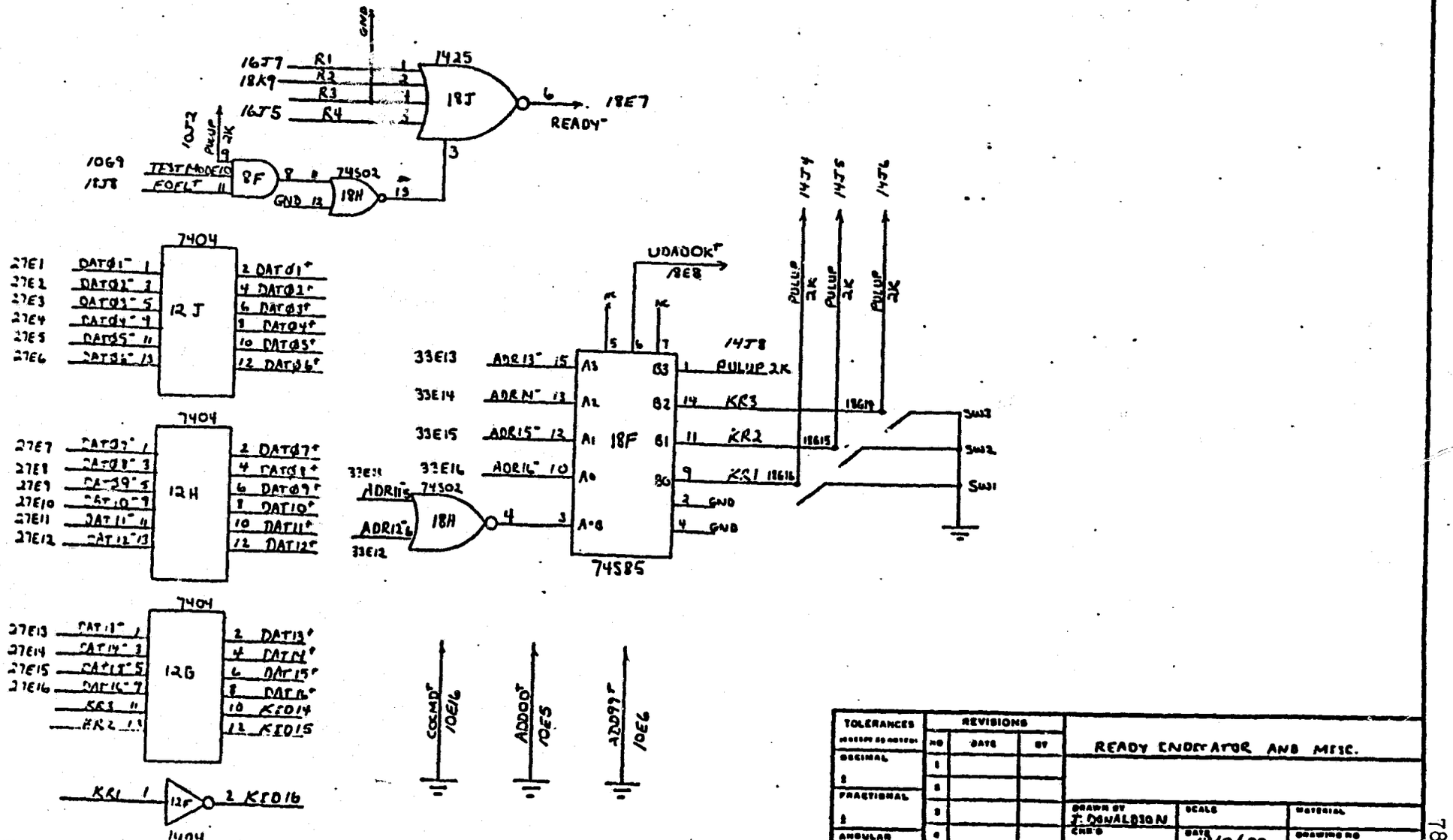

TOLERANCES	REVISIONS			READY ENDICATOR AND MISC.		
DECIMAL	NO	DATE	BY			
FRACTIONAL						
ANGULAR				DRAWN BY J. DONALDSON	SCALE	MATERIAL
				CHK'D	DATE 11/9/77	DRAWING NO L80-11
				ISSUED	APP'D	

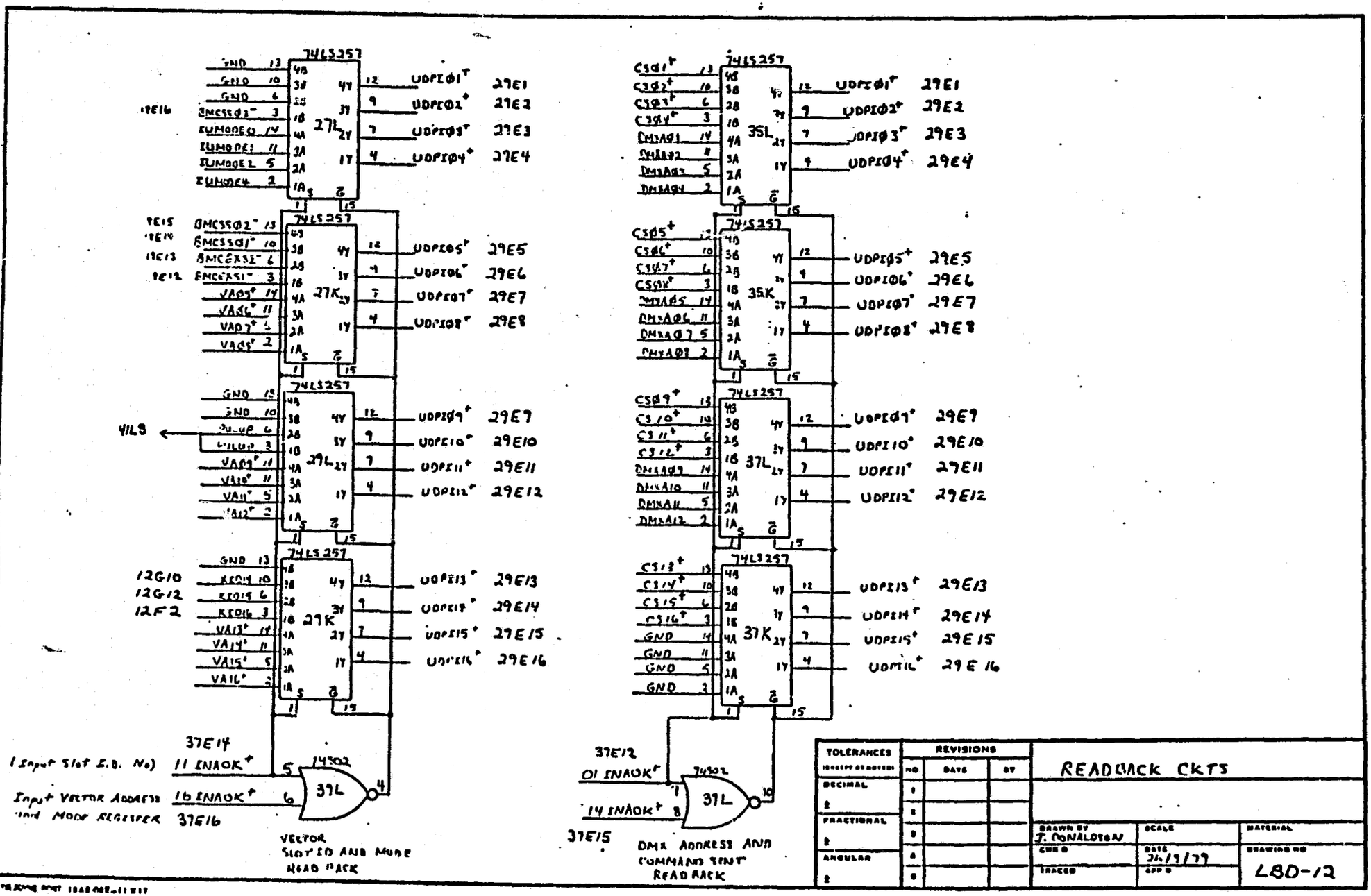
74LS257
27L
27K
35L
35K
37L
37K
UDPIØ1+ 29E1
UDPIØ2+ 29E2
UDPIØ3+ 29E3
UDPIØ4+ 29E4
UDPIØ5+ 29E5
UDPIØ6+ 29E6
UDPIØ7+ 29E7
UDPIØ8+ 29E8
UDPIØ9+ 29E9
UDPI10+ 29E10
UDPI11+ 29E11
UDPI12+ 29E12
UDPI13+ 29E13
UDPI14+ 29E14
UDPI15+ 29E15
UDPI16+ 29E16
12G10
12G12
12F2
4LS
37E14
11 INAOK+
16 INAOK+
37E16
VECTOR SLOT ID AND MODE READ BACK
37E12
01 INAOK+
14 INAOK+
37E15
DMA ADDRESS AND COMMAND BIT READ BACK
TOLERANCES
REVISIONS
READBACK CKTS
DRAWN BY J. DONALDSON
DATE 3/9/79
DRAWING NO L80-12

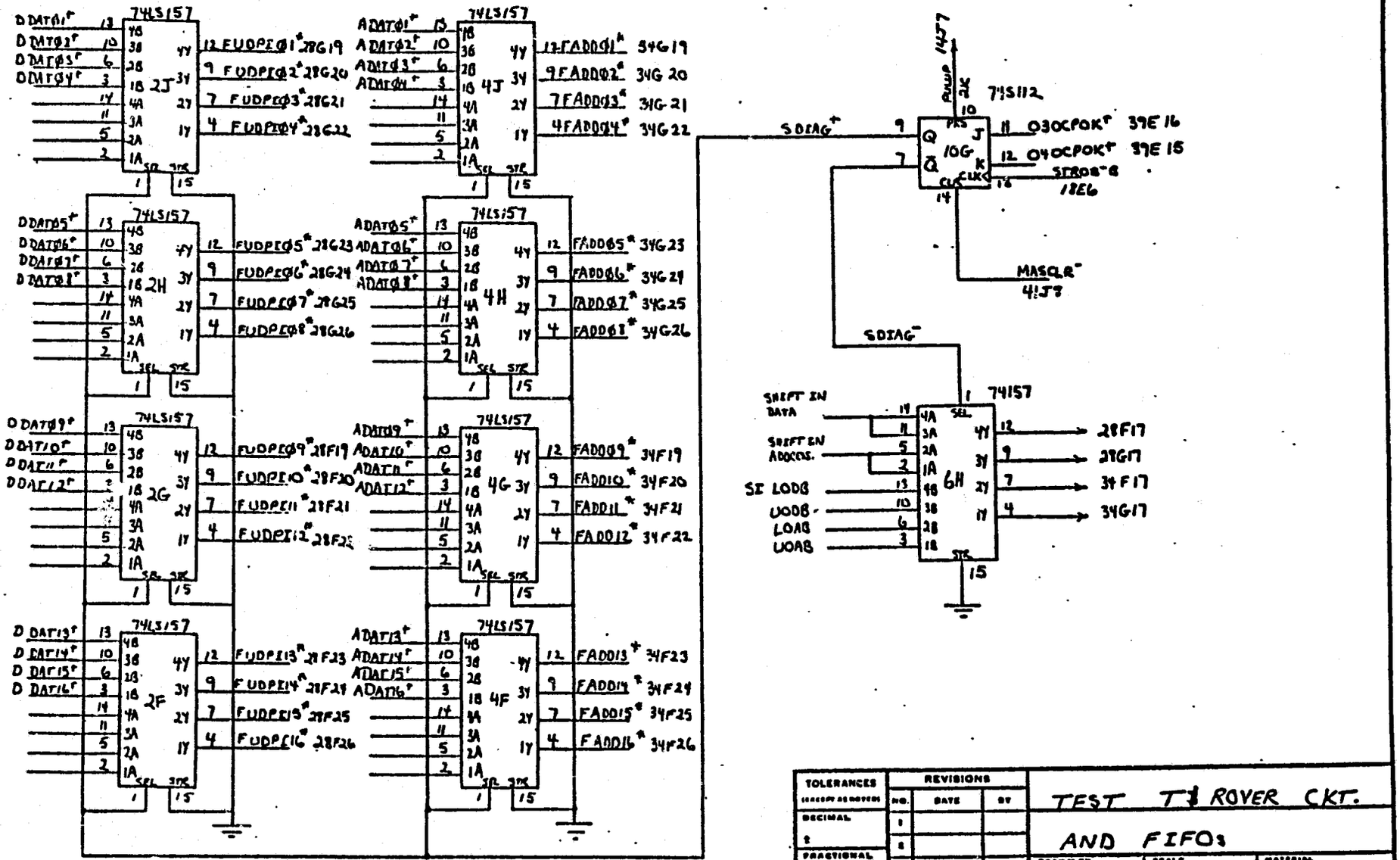

TOLERANCES	REVISIONS			TEST T³ ROVER CKT. AND FIFOs		
DECIMAL ±	NO.	DATE	BY			
FRACTIONAL ±						
ANGULAR ±				DRAWN BY T. DONALDSON	SCALE	MATERIAL
				CHK'D	DATE 29/10/79	DRAWING NO LSD-13
				TRACED	APP'D	

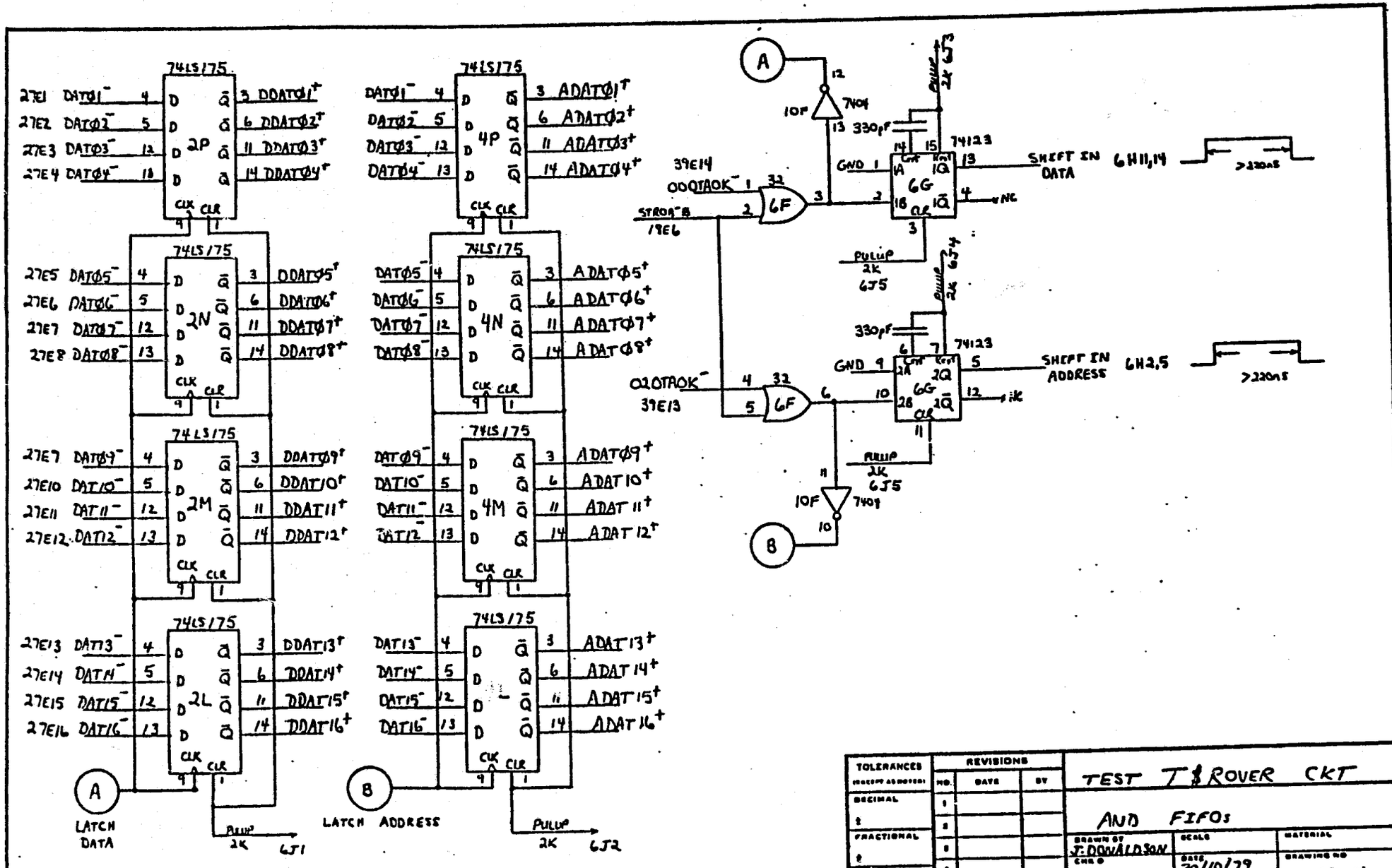
74LS175
2P
2N
2M
2L
4P
4N
4M
4L
LATCH DATA
LATCH ADDRESS
A
B
7404
74123
6G
6F
330pF
2K
SHEFT IN DATA
SHEFT IN ADDRESS
>220nS
GND
NC
TOLERANCES
REVISIONS
TEST T$ROVER CKT
AND FIFOS
DRAWN BY J. DONALDSON
DATE 30/10/79
DRAWING NO L6D-14

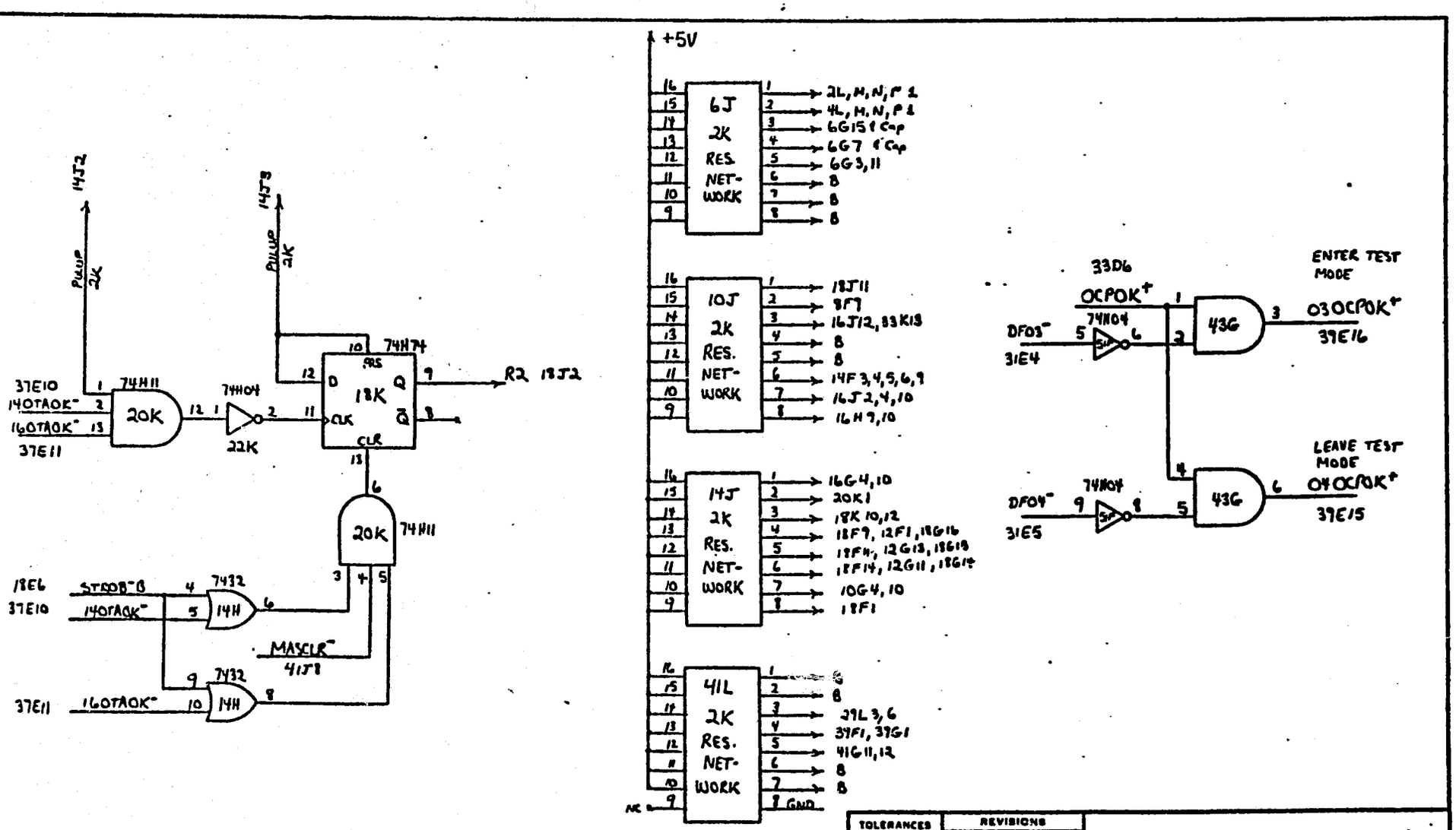

TOLERANCES	REVISIONS			READY CKT FOR OTA146X' AND OTA166X' AND MISC.		
DECIMAL ±	NO	DATE	BY			
FRACTIONAL ±						
ANGULAR ±				DRAWN BY T. DONALDSON	SCALE	MATERIAL
				CHK'D	DATE 7/11/79	DRAWING NO LBD-15
				TRACED	APP'D	

Appendix 5.3
Circuit Diagrams for Data Emulator

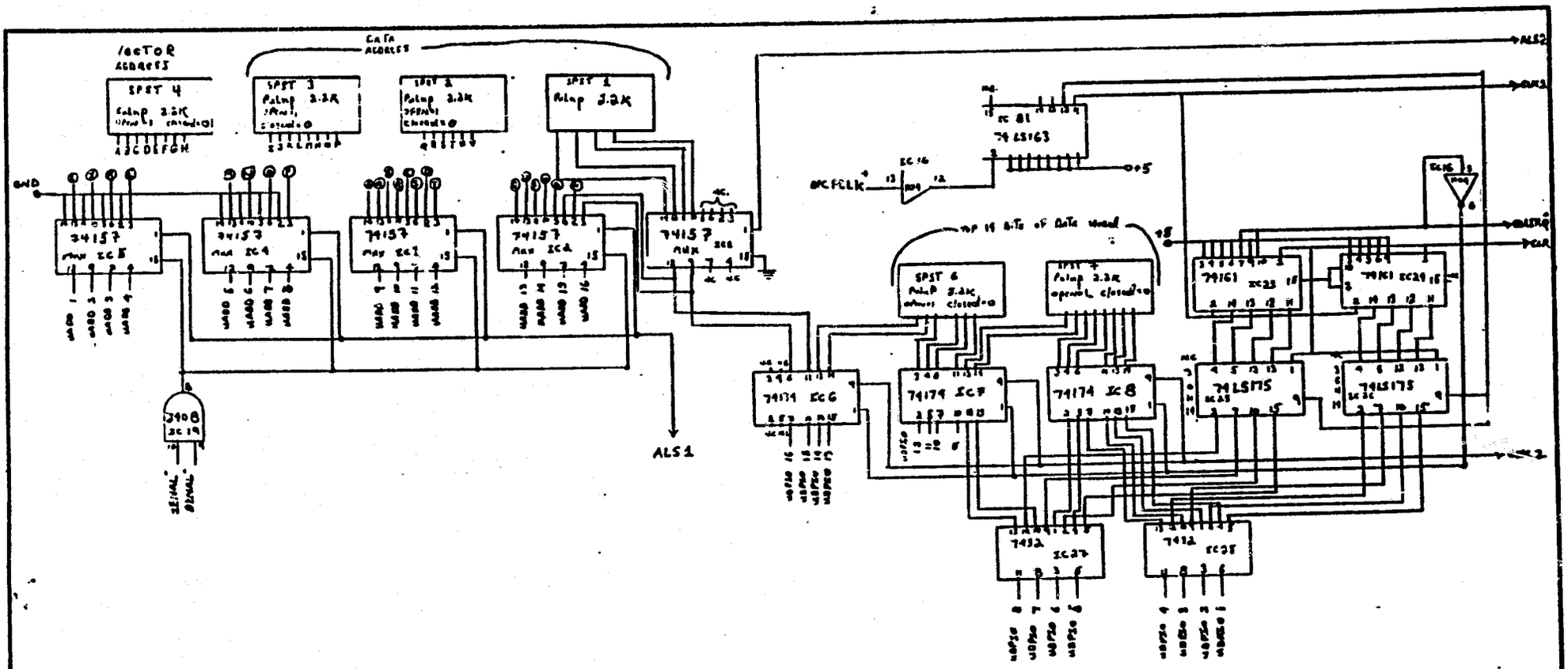

ALS = ADDRess Line SelecT

TOLERANCES	REVISIONS		
DECIMAL ±	NO.	DATE	BY
FRACTIONAL ±			
ANGULAR ±			

DRAWN BY R. Miller
CHK'D
TRACED
SCALE
DATE 10/3/79
APP'D J. DONALDSON
MATERIAL
DRAWING NO

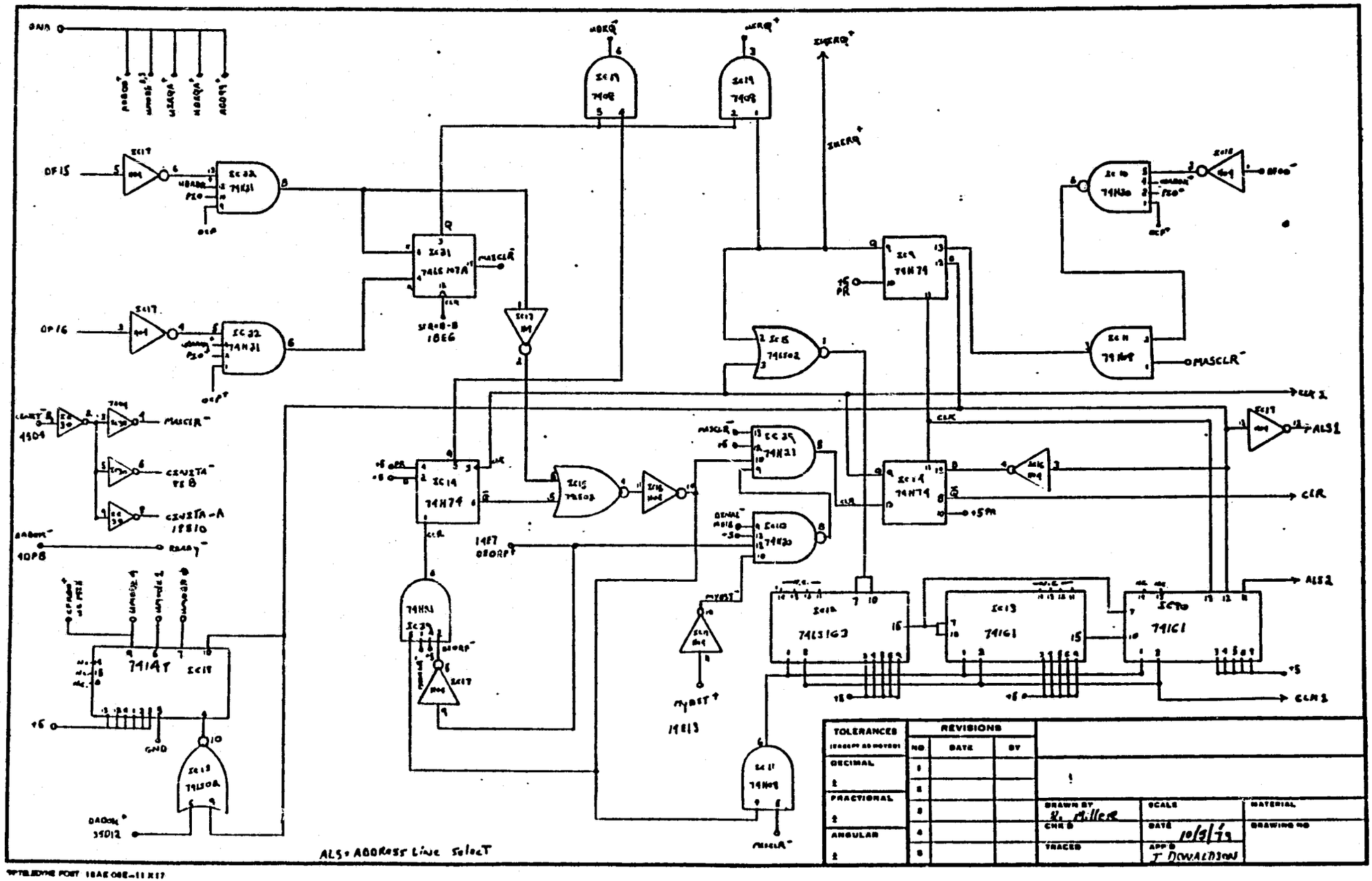
ALS = ADDRess Line Select
TOLERANCES
REVISIONS
NO
DATE
BY
DECIMAL
FRACTIONAL
ANGULAR
DRAWN BY
CHK'D
TRACED
SCALE
DATE
APP'D
MATERIAL
DRAWING NO